ELSEVIER

Bioinspired design toward nanocellulose-based materials

Xianhui Zhao [1,*], Samarthya Bhagia [2], Diego Gomez-Maldonado [3], Xiaomin Tang [4], Sanjita Wasti [5], Shun Lu [6], Shuyang Zhang [7], Mahesh Parit [8], Mitchell L. Rencheck [9], Matthew Korey [9], Huixin Jiang [4], Jiadeng Zhu [10], Xianzhi Meng [7], Meghan E. Lamm [9], Katie Copenhaver [9], Maria S. Peresin [3], Lu Wang [8], Halil Tekinalp [9], Guang Yang [4], Vipin Kumar [9], Gang Chen [11], Kashif Nawaz [12], X. Chelsea Chen [4], Uday Vaidya [5,9], Arthur J. Ragauskas [2,7,13], Erin Webb [1], Douglas J. Gardner [8], Ping He [14], Ximin He [14], Kai Li [13,*], Soydan Ozcan [9,*]

[1] Environmental Sciences Division, Oak Ridge National Laboratory, Oak Ridge, TN 37830, United States
[2] Biosciences Division, Oak Ridge National Laboratory, Oak Ridge, TN 37830, United States
[3] Sustainable Bio-based Materials Laboratory, Forest Products Development Center, College of Forestry, Wildlife and Environment, Auburn University, Auburn, AL 36832, United States
[4] Chemical Sciences Division, Oak Ridge National Laboratory, Oak Ridge, TN 37830, United States
[5] Tickle College of Engineering, University of Tennessee, Knoxville, TN 37996, United States
[6] Department of Agricultural and Biosystems Engineering, South Dakota State University, Brookings, SD 57007, United States
[7] Department of Chemical and Biomolecular Engineering, University of Tennessee, Knoxville, TN 37996, United States
[8] AdvancedStructures and Composites Center and School of Forest Resources, University of Maine, Orono, ME 04469, United States
[9] Manufacturing Science Division, Oak Ridge National Laboratory, Oak Ridge, TN 37830, United States
[10] Smart Devices and Printed Electronics Foundry, Brewer Science Inc., Springfield, MO 65806, United States
[11] Department of Civil & Environmental Engineering, Florida State University, Tallahassee, FL 32310, United States
[12] Buildings and Transportation Science Division, Oak Ridge National Laboratory, Oak Ridge, TN 37830, United States
[13] Department of Forestry, Wildlife, and Fisheries, Center for Renewable Carbon, The University of Tennessee Institute of Agriculture, Knoxville, TN 37996, United States
[14] Department of Materials Science and Engineering, University of California Los Angeles, Los Angeles, CA 90095, United States

Nature provides lots of inspiration for material and structural design for various applications. Deriving design principles from the investigation of nature can provide a rich source of inspiration for the development of multifunctional materials. The bioinspired design templates mainly include mussels, nacre, and various plant species. As a sustainable and renewable feedstock, nanocellulose can be used to fabricate advanced materials with multifunctional properties through bioinspired designs. However, challenges and opportunities remain for realizing the full potential in the design of novel materials. This article reviewed recent development in the bioinspired nanocellulose based materials and their application. This article summarizes the functions (e.g., surface wetting) and applications (e.g., composite) of bioinspired nanocellulose-based materials. The bioinspired design templates are discussed along with strategies, advantages, and challenges to the development of synthetic mimics. Additionally, mechanisms

* Corresponding authors.
E-mail addresses: Zhao, X. (zhaox@ornl.gov), Li, Kai (lik1@ornl.gov), Ozcan, S. (ozcans@ornl.gov).

 https://doi.org/10.1016/j.mattod.2023.04.010

and processes (e.g., chemical modification, self-assembly) leading to biomimetic design are discussed. Finally, future research directions and opportunities of bioinspired nanocellulose-based materials are highlighted.

Keywords: Bioinspired; Nanocellulose; Multifunction; Polymer; Composite

Introduction

Functional natural materials form a hierarchical nanostructured architecture by self-assembling in a variety of ways including self-folding or forming complex arrangements with other polymers and salts in an aqueous cellular matrix. These nanostructures can further assemble to macrostructures, forming complex systems with unique mechanical, optical, and other physiological properties. Natural materials continue to inspire the design of new functional engineered materials aiming to simulate properties of materials found in nature [1].

Biological materials can be used as inspiration sources for the design of biobased materials. For example, mussels exhibit remarkable strength and can survive in fierce waves by sticking to wet rocks through secreted byssus [2,3]. Nacre in mollusk shells has attracted extensive attention for its exceptional properties, such as its light weight and unique combination of strength and toughness [4–6]. The scaled skin of teleost fish particularly displays strength, flexibility, resistance to penetration, and light weight. It consists of spatially arranged scales attached to a thin flexible dermis layer [7]. Squid beak is strong gradient biological fiber composite with a fully organic composition. The beak has a stiff tip and is one of the hardest known organic materials, with an elastic modulus of 5 GPa, whereas the modulus of squid's connecting tissue is only 50 MPa [8]. Therefore, the bioinspired design towards high-performance materials has attracted the attention of many researchers recently.

Abundancy and commercial availability are important factors for the introduction of engineered biobased materials to different markets. Because of its large availability, cellulose presents a competitive advantage and has been widely used and studied throughout the years for paper, packaging, and other commodities [9]. Cellulose is the main structural polysaccharide in plant cell walls and is also present in algae matrices, bacterial biofilms, and some animal extracellular matrices [10]. Cellulose consists of a linear homopolysaccharide of β-D-glucopyranose unit. Its abundance and commercialization from wood pulp production makes it a feasible and sustainable material for product development. The linear chains of cellulose assemble into nanoscale fibrils with crystalline and amorphous regions. These fibrils are mainly held together by hydrogen bonding, resulting in structures that can interact with other materials through van der Waals, hydrophobic, and electrostatic forces [11]. Nanocellulose refers to nanostructured cellulose in this study, also called cellulose nanomaterial, which covers both cellulose nanofibril (CNF) and cellulose nanocrystal (CNC; i.e., cellulose nano-whisker [CNW]). CNCs are typically produced by acid hydrolysis. CNFs are hygroscopic nanoscale particles which are insoluble in water or traditional solvents [12], thus holding great potential for biomedical applications that require positive interfacial interaction with living organisms.

CNFs are most commonly obtained from lignocellulosic biomass through mechanical refining or grinding, chemical or enzymatic treatments, homogenization or microfluidizing, or combinations thereof [9,13]. CNFs have an ultrahigh aspect ratio (approximately 10–100 nm wide and up to several micrometers long), superior mechanical performance (axial tensile strength around 3 GPa), high surface area, efficient biodegradability, low weight, and global abundance. CNFs have been used as reinforcing fibers in polymer composites [13–15]. In addition, CNFs have good potential in other applications, including adhesive binders, flexible electronics, automotive, packaging, infrastructure, building, and separation media [9].

CNFs assemble with other biopolymers in the cell wall, usually hemicelluloses, lignin, and pectin [10]. Additionally, CNFs can be hydrolyzed to obtain CNCs. The different aspect ratios and crystallinity of CNCs from CNFs provide them with different mechanical and optical properties, making them suitable for certain applications (e.g., composites, adhesive binders) [16]. Another important property of cellulose is its chirality [17]; the self-assembly of the individual chains into the nanoparticle results in a positive chirality, with a torsional period of ~232 nm, which can vary with the functional groups present on the surface [17,18]. This chirality is relevant for the interaction of nanocellulose with light because it dictates the optical properties of CNC-based assemblies such as films [19,20].

CNCs can extract moisture from the atmosphere. In addition, as nanocellulose-based products, CNCs have exceptional physical and biological properties, such as high crystallinity degree, large specific surface area, high aspect (length/diameter) ratio, high thermal resistance, good mechanical properties, an abundance of surface hydroxyl groups, biodegradability, and biocompatibility [21]. Additionally, the self-alignment of cellulose fibrils results in an inherent piezoelectric nature, in which a mechanical stress translates into a change of the electrical polarization of the material [22]. This property has been studied mostly in CNC-based films because it is enhanced by the more rigid crystals [23]. However, this property is retained in CNF, opening the possibility for developing cellulose nanofibril-based electroresponders [22,24].

The inclusion of cellulose into the nano- and colloidal material fields has created several new relevant applications and products. The remarkable mechanical and optical properties, renewability, and abundance make nanocelluloses especially interesting as reinforcing agents for polymeric matrices [25,26]. These properties are especially relevant as the need for biobased and green materials grows to tackle pollution and demand of fossil-based materials. The versatility of products in which nanocelluloses can be processed—including fiber yarns [27], films, hydrogels, and aerogels, as well as the variety of surface

functionalization and derivates available—make them interesting for numerous applications such as drug delivery, efficiency-enhanced fertilizers, water treatment, tissue engineering, and additive manufacturing [28].

Properties such as their amphipathic nature, anisotropic dielectric distribution, piezoelectric and optical properties, pH and thermal response, and nanocellulose assembly into films with tunable permeability have made nanocelluloses promising for engineered materials [29,30] in areas such as active packaging, self-cleaning materials, energy storage, solar cells, adhesives, electronics, shape memory materials, and bioactive sensors [31,32]. The discussed properties and product development opportunities of nanocelluloses have fueled research and innovation efforts and working toward social acceptance and legislation is imperative for nanocelluloses to be used in common daily applications.

Because of the highly oriented molecular chains, strong inter-/intra-molecular hydrogen bonding, and high crystallinity, nanocellulose exhibits superior mechanical properties with a predicted modulus of 10–50 GPa and strength of 1–8 GPa [33]. Nanocellulose-based materials have demonstrated the capacity of reinforcing polymeric matrices in the same manner, in which they reinforce the native lignin and hemicellulose matrix in the cell wall [15,34,35]. In addition to providing structural functions, cellulose fibrils also provide resistance to osmotic pressures in the cell wall, rigidifying it and providing turgor to the membranes. Fibrillar angle and molecular weight significantly affect the magnitude of both properties [36]. However, many challenges that limit the global commercialization of nanocelluloses still remain. One of the most remarkable challenges is related to the wide variation in chemical composition, size, and certain properties that depend on the starting material [37]. Such variability impairs reproducibility of the results found in lab-scale products and mass production. In addition, nanocelluloses are mainly available in water-based suspensions with solid contents around 2–4 wt% [38], requiring the transportation of large amounts of water to processing facilities. Many industrial stakeholders are currently working on addressing the scaling of the process while determining pathways to decrease water content and maintain the dispersion of the nanocelluloses. Various chemical modification strategies, inspired by nature, are potential to be helpful in specific high-performance applications.

This review article is driven by the wide variety of applications that nanocelluloses have, and the possibility to generate engineered materials that can achieve performance comparable to those of naturally occurring materials. Thus, this article examines the new research developed in assembly variations, functionalization, and composite formulation. Also, this work aims to review recent possible bioinspired functionalities including self-cleaning, adhesion, stimuli response, shape memory, sensing, and actuation. An outlook of the advantages and strategies than can be analyzed for new and better products will also be provided.

Bioinspired design sources and strategies

Nanocellulose is made from repeating β-(1,4)-linked D-glucose units from a molecular level, and there are many OH groups on the surface of nanocellulose. The unique chemical structure of nanocellulose provides a chemistry base for its applications in biomimetic applications. The hydrogen bond is critical in the biological system and has been applied in biomimetic applications [39]. The abundant OH groups of nanocellulose can form a strong hydrogen bond with various molecules. These OH groups can be functionalized through multiple chemical reaction mechanisms, such as sulfonation, oxidation, esterification, etherification, silylation, urethanization, amidation, and polymer grafting, to impart desired properties to nanocellulose [33]. Moreover, nanocellulose can form ionic interactions with charged compounds and coordination interactions with metal ions [40]. These different interactions are widely found in the biological system and play significant roles in their properties. For instance, interfacial bonding (e.g., hydrogen bond, π–π interaction, cation–π attraction, metal coordination) in dopamine-based chemistry is one reason for the strong adhesion and toughness of mussels [41–43]. These interactions have also been used in biomimetic applications, such as adhesion, stimuli-responsive materials, and coatings. In this section, bioinspired design sources are reviewed, and design strategies are discussed.

Mussel, nacre, and other sources

Deriving design principles from the investigation of biological systems can provide a rich source of inspiration for the development of multifunctional materials. This section summarizes the current understanding of primary examples of biological materials as inspiration sources for the design of cellulose-based materials, including inorganic/organic composites (e.g., mussel, nacre, fish skin), organic/organic composites (e.g., squid beak, human skin, resilin), and other sources such as muscle, fungus-like oomycetes, and the natural hemostasis process [44]. Diverse solutions are available for the engineering of promising new bioinspired cellulose-based materials with intriguing properties.

The mussel byssal threads exhibit remarkable strength and extensibility, crosslinking, and strong adhesion (Fig. 1A). These intriguing properties have been attracting researchers to incorporate mussel-inspired chemistry into cellulose-based materials to make them functional and extend their applications [2,3]. Researchers isolated nine mussel foot proteins and discovered that no less than six mussel foot proteins containing dopa residues, a modified amino acid with two hydroxyl group attached to tyrosine [45–47]. Dopa residues have been implicated as one of the principal reasons for robust interfacial bonding [48,49]. The bonding strategies of dopa to diverse surfaces include hydrogen bonds, π–π interactions, cation–π attraction, metal coordination, and Michael addition (Fig. 1B) [41–43]. Furthermore, dopa contributes to cohesion of byssus through coordination with metal ions. The strong but sacrificial bonds increase energy dissipation by repeatedly breaking and reforming when bearing loads [50].

Nacre is essentially a ternary composite of calcium carbonate (more than 95 vol%), nanofibrillar chitin, and protein [51]. The layers of aragonite platelets, with a thickness of 200–900 nm and a diameter of 5–8 um, are held together by an organic layer of chitin network and soft protein with a thickness of 10–50 nm (Fig. 1C and 1D) [51]. Such layering of soft and stiff materials at the nanoscale offers a good balance of strength and toughness.

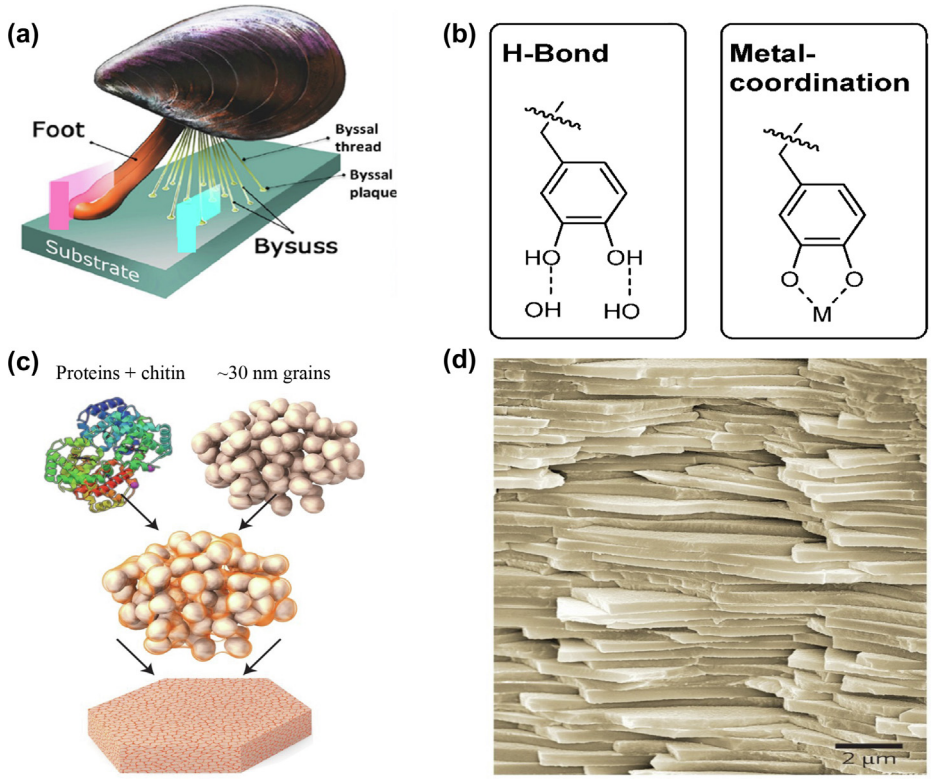

FIGURE 1

Schematic of mussel and nacre. (A) mussel and its byssus; (B) mussel-inspired chemistry (e.g., H-bond, metal coordination) [3]; (C) nacre platelet composed with $CaCO_3$ nanograins glued together by a biopolymer; and (D) nacre is a brick and mortar structure of mineral platelets [51].

The multilayered composite systems based on stiff materials with soft interlayers (e.g., silica and polymer, ceramic polymer composite) exhibit toughness superior to that of the constituent materials. Therefore, the layering of stiff and soft materials leads to considerable gains in toughness. Most mineral components provide overall stiffness and hardness. Despite the small amount of organic materials in nacre, these materials play a large role in increasing toughness because of their enormous interface area. The interfaces force cracks to be deflected and permit crack bridging, platelet and fiber sliding, and pullout. The other possible toughening mechanisms are sacrificial bonds in the organic layers, presence of preexisting mineral bridges, microfracture of mineral bridges, plastic deformation of platelets at the nanoscale, and platelet interlocking at the microscale. These mechanisms lead to a 40-fold increase in toughness for nacre compared with its majority-brittle constituent aragonite [52].

Under high–strain rate uniaxial compression, partial dislocation emission and deformation twinning also result in higher fracture strength of nacre's aragonite platelets [53]. Li et al. [54] mentioned that the deformability of aragonite platelets together with the crack deflection, aragonite platelet slip, and organic adhesive interlayer results in a 1000-fold increase in toughness over its constituent materials [55]. Another report demonstrated a new energy dissipation mechanism hidden in nacre and activated only upon dynamic loading, where the crack straightly impinges the aragonite platelets instead of propagating along nacre's biopolymer interlayers [56].

Seashells are highly organized nanocomposites designed to be extraordinarily tough while remaining hard and strong. The shell's basic building blocks (i.e., the nanowire-like third-order lamellae) are brittle single-crystal aragonite [57,58]. The individual aragonite platelets consist of millions of nanosized particles [59]. The biopolymer between the nanograins allows enough space for certain grains to rotate. The grain rotation and deformation are responsible for the high deformability of individual aragonite platelets. Such individual aragonite platelets with particle architecture avoid a crack rigidly invading the aragonite platelet through a special cracking mechanism that favors local buffering [60]. In addition to the lamellar architecture, the morphogenetic puzzle of interlocking bivalved shells has been studied by mechanic models [61]. The revealed interlocking mechanism has been adopted in several engineered materials. Interlocking is an important mechanism that contributes to joint mechanical property enhancement [62,63].

Fish skin is another mineralized biological source from which functional cellulose materials can be developed [64]. The scale is a cross-ply layered composite that comprises collagen fibrils and is mineralized with 16–59 wt% hydroxyapatite (Fig. 2A-C) [7]. The outer layer is usually hard and has a higher mineral content than the inner layer. This cross-ply collagen structure of each scale, the spatial arrangement of the scales, and the interactions of the scales with the dermis layer and between neighboring scales provide the scaled skin with remarkable strength along multiple directions, along with flexural compliance.

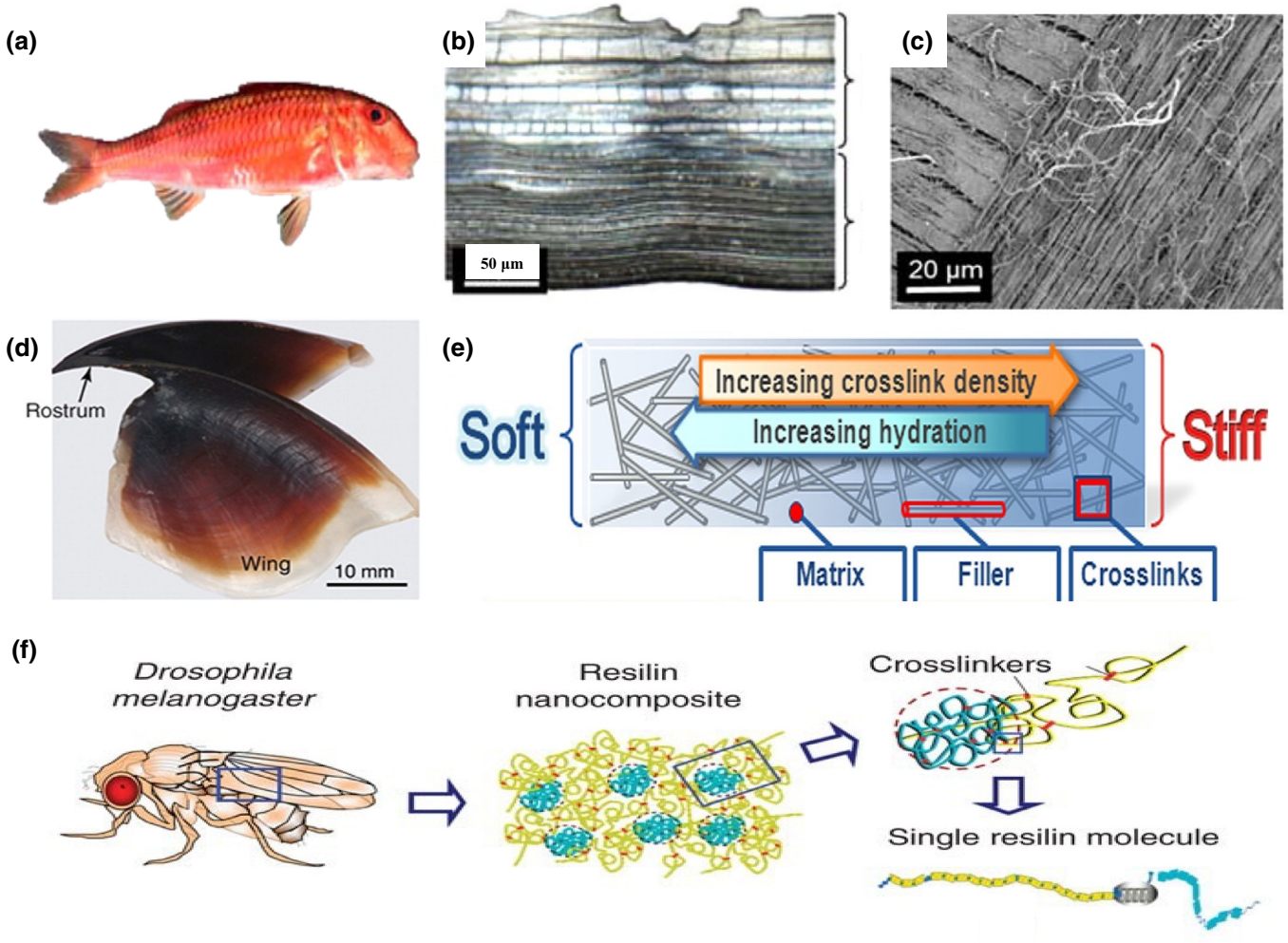

FIGURE 2

The structures of a fish skin, squid beak, and fruit fly resilin. (A) A whole fish; (B) cross-section structure of a fish scale; (C) cross-ply collagen structure showed by the top view of a scale [64]; (D) the squid beak, including the rostrum and the wing; (E) schematic overview of proposed mechanisms of the mechanical gradient structure [65]; and (F) the resilin exists in as an amorphous crosslinked nanocomposite [66].

Squid beak is strong natural fiber composite [8]. To bridge these two extremely mechanically mismatched tissues, the remaining part of the beak exhibits a gradient in stiffness spanning 2 orders of magnitude from the tip to the base (Fig. 2D). The gradient originates from the changes in the amount of crosslinking between histidyl groups and dopa in the protein matrix, and water content across the wing (Fig. 2E). The region close to the tip has more protein (40%–50%) and less water (20%) [52]. Moving toward the base, the protein is gradually replaced by water and the base area contains up to 70% water.

The lotus plant (*Nelumbo* genus), a lignocellulosic inspirational organism, is highly regarded because of its ultrahydrophobic leaves [67] and unique lotus silk [68]. The self-cleaning behavior observed on these pound plants is derived from the micro- and nanostructure of protrusions and valleys that the cell walls form, aided by nanoparticles of a wax-like material formed randomly on the surfaces [69]. The random papillae structures minimize the contact that water drops would have with the plant, allowing for air trapped in the spaces to push the water and allowing them to roll out. The epicuticular wax decreases the surface area and slicing angle, maximizing the hydrophobic character [70]. Here, cellulose impact is mostly present in its structural component as a part of the cell walls forming the structures in the leaf, which demonstrates the versatility of this biobased material. A more direct impact of cellulose is in the lotus silk, which is the cellulose fibers that form the stem of the lotus. These fibers have a hierarchical growth that mimics a spiral conferring stretchability and good energy dissipation [71] without a clear lumen. As the plant matures, the fiber becomes smoother and acquires wax conglutinations, increasing its diameter and organization [72]. Moreover, when heated, the mechanical properties of this material can be further improved [73], demonstrating the potential for new processable products.

Sea cucumbers (*Cucumaria frondosa*) present a sudden 10-fold increase in mechanical stiffness when in danger [74]. This response is possibly due to the reversible crosslinking of the collagen fibers in the extracellular matrix of its connective tissue by the glycoprotein stiparin [75] and tensilin [76]. The reversibility of these bridges is done by another inhibitor glycoprotein that is activated with the stimuli off [76]. Despite the advancements

in understanding this underlying mechanism, there are still many unknowns. Nevertheless, reversible stimuli-responsive materials are being developed using other simpler driving mechanisms such as hydrogen bonding [76,77], water presence [78], and heat [79], as well as more complex mechanisms such as chemo presence [74] and cyclodextrin inducing treading [80]. These biobased actuator materials are usually in wet applications, allowing for bio-interfacing to develop smart and responsive systems, and demonstrating the advantages of bioinspiration for high-end value-added products.

Resilin is a rubber-like insect protein and exists as a crosslinked highly amorphous hydrogel (Fig. 2F) [66]. It features high resilience (>95%), large strain (>300%), and low moduli (0.1–3 MPa) [81]. The possible sources of these properties include long polymer chain length, outstanding chain flexibility, and well-defined crosslinks between specific amino acids, which offer the routes to reproduce its mechanical property for synthetic materials [82].

Human skin is another non-mineralized composite with remarkable toughness that has inspired the design of new cellulose materials [83,84]. The dermis (the principal structure for mechanical properties of skin) consists of collagen fibers dispersed in an elastin matrix. The toughness of human skin mainly originates from fibril straightening, reorienting, polymer chain and chemical bond stretching and breaking, and delaminating when bearing load. Human skin also offers nonlinear elasticity, being soft at small strains and stiff at large deformations. The property is achieved through the combination of semirigid collagen nanofiber and elastomeric elastin fibers that are chemically integrated in the network.

Human muscles are natural flexible actuators that can efficiently transport nerve impulses and perform diverse deformations with outstanding shock-absorbing ability. Muscles can generate electrical currents by controlling ion channels and trigger an action potential to travel along a cell membrane quickly. The actuation is then triggered by the release of calcium ions when the potential is transmitted to the muscle junction. This indicates the importance of the effective release and conduction of ions in human muscles and inspired researchers to find solutions to improve actuation performance [85]. In summary, because of the remarkable properties (e.g., mechanical strength, adhesion), mussel, nacre, fish, squid beak, resilin, human skin, and human muscle have inspired the design of nanocellulose-based materials. The application of knowledge of biological materials would help resolve technical issues.

Bioinspired design strategies

Biomineralization

Table 1 shows the bioinspired design strategies in diverse research results. Biomineralization is the study of biologically produced materials and the processes that lead to their formation [86]. Biomineralization can mimic the hierarchical structure and chemical components of bone and dentin. Mineralized nanocellulose mimics the hierarchical structure and chemical components of bone and can be used to produce a candidate hybrid composite for the repair and/or regeneration of damaged bones or teeth [87]. The production and properties of these materials involve a large number of biological macromolecules—including proteins and polysaccharides—that maintain strict control of the process, even in conditions that are not thermodynamically favorable for their nucleation and growth [88]. Examples of natural minerals include carbonates [89], such as biogenic calcium carbonate (calcite) found in mollusk mantles and egg shells; and phosphates [90], including calcium phosphate, the major structural component in bones and teeth. Other examples include gypsum (jellyfish larvae), silica (sponge), and magnetite (magnetotactic bacteria).

Significant efforts have been undergone to understand and replicate *in vivo* biomineral synthesis for numerous applications using synthetic polymer composites. However, replicating nano- and microstructural features of the extracellular matrix while maintaining biocompatibility and achieving mechanical properties resembling those of natural hard tissues has remained challenging. The use of cellulose as a base component for fabricating hydrogels and other constructs for biomedical applications has gained significant attention in recent years; however, the mechanical properties of nanocellulose hydrogels are limited, impeding their applicability in hard tissue regeneration. For example, researchers have explored cellulosic hydrogels with hydroxyapatite, nanocellulose, and other calcium phosphates in recent years to achieve hard tissue regenerative scaffolds [115,116], but these structures do not typically match the innate properties of natural hard tissues [117].

Recent work showed that the use of oxidized CNF-containing hydrogels could form materials with highly ordered and mineralized nanostructures and achieved comparable hardness values to human dentin and mouse cortical bone, though elastic modulus values remained significantly reduced [87]. Qi et al. [87] fabricated a bioinspired composite made of nanocellulose that was mineralized with hydroxyapatite nanocrystals. Fig. 3A-D shows a schematic illustration of fabricating the mineralized aligned CNF composite. The molecular assembly of materials can provide nanocompartments and enable mineralization. The mineralization can help overcome the low mechanical properties of cellulose-based materials and improve the bioactive properties [87].

Mohammadi et al. attempted to mimic the dactyl club of the peacock mantis shrimp by generating highly organized biocomposites made of CNCs mixed with genetically engineered protein matrices containing cellulose-binding modules to harden, strengthen, and stiffen apatite crystals (Fig. 3E) [91]. The protein–protein interaction and the molecular network create interlocking regions. The researchers achieved a graded microstructure with a correlated mechanical gradient that closely resembled those observed in natural biomineralized composites. Farhadi-Khouzani et al. developed nanocellulose and calcium carbonate-based composites through layer-by-layer assembly to imitate nacre [6]. The researchers achieved a Young's modulus in excess of biogenic nacre owing to crack deflection and trapping by the crystals and organic layers, but they did not achieve the desired hardness or fracture toughness. The resulting materials have potential applications in buildings and packaging.

Coating, assembly, and dispersity strategies

Several plants and animals incorporate superhydrophobic surfaces with a water contact angle of more than 150°, including tri-

TABLE 1

Bioinspired design strategies in diverse research results.

Target performance	Composition and resultant material	Design strategy	Design source	Ref.
Reinforced composite	Cellulose-based biocompatible scaffolds with target mechanical performance	Biomineralization	Human dentin and mouse cortical bone	[87]
	Organized cellulose-protein binding composite		Dactyl club of the peacock mantis shrimp	[91]
	Calcium carbonate–based composite on nanocellulose matrix		Nacre	[6]
	Montmorillonite platelet/CNF/PVA composite	Assembly	Natural nacre in mussels	[92]
	CNF and CMC with ACC and PAA		Crustacean exoskeleton	[93]
	Functionalized CNC crosslinked with a copolymer through UV irradiation		Humboldt squid beak	[94]
	CNC film (wood-derived CNCs and tunicate-derived CNCs)		Helicoidal microstructure of a bone, crustacean shells, and ivory	[95]
Reinforced composite; high thermal stability	Composite hydrogel with highly oriented CNF and TiO_2		Multiscale architecture of nacre	[96]
Reinforced composite; flame resistance and high thermal stability	Black phosphorus functionalized with hydroxyl groups (BP − OH)/CNF composite		Brick-and-mortar microstructure of nacre	[97]
Conductive, electrically insulating, flexible, superhydrophobic, self-cleaning	CNF/OH − BNNS film		Lotus leaf and nacre (brick-and-mortar)	[98]
High adhesion	CNF/dopamine/Fe^{3+} composite		Marine mussel byssal threads	[2]
Shape memory material	CNW-reinforced ethylene oxide–epichlorohydrin polymer		Dermis of sea cucumbers	[99]
	CNW-reinforced polyurethane		Sea cucumber dermis	[100]
Structural colors	Copolymer blended with CNC		Beetle shells and butterfly wings	[101]
Flexible liquid sensor	CNF/carbon nanotube nanocomposite		Wood-like multi-component structures	[102]
Strain sensor	Cellulose-based paper		Human skin and rodent	[103]
Actuation	Nanocellulose-based colloidal liquid metal		Soft tissue	[104]
	Poly(vinyl alcohol-co-ethylene) substrate with a hydrophilic nanocellulose coating		Motile plant	[105]
	Hydrogel from chitosan and nanocellulose		Plant tissues	[106]
Biomimetic foam	CNF/starch composite		Parenchyma cells	[107]
Superhydrophobic	Silane-modified CNF microparticle	Coating/modifying	Hierarchical surface of lotus leaf	[108]
	CNF aerogel microsphere–coated filter paper		Leaf-like structured surface roughness	[109]
	Copper iodide–modified cellulose paper		Rose petal	[110]
	Nanocellulose aerogel carrier with load-carrying ability		Water strider legs	[111]
Water resistance, reinforcement	CNF/dopamine/montmorillonite nanocomposite		Mussel adhesive protein	[112]
Water resistance	Core-shell CNF (amylopectin-coated CNF)–containing nanocomposite		Plant cell wall	[113]
Flame resistance	BNNS-p-APP and CNF composite		Nacre-like microstructure	[114]

ticum and lotus plant leaves, the surface of duck feathers, and insect cuticles [118–121]. A recent review by Bayer provides a comprehensive review of superhydrophobic nanocellulose coatings, some of which are bioinspired [122]. In addition to this work, Wang et al. developed bioinspired regenerative, nanocellulose, superhydrophobic coatings inspired by the papillae structure of the lotus leaf [123]. Although research in this area is limited, there could be numerous applications for development in terms of biocompatible and environmentally friendly anti-fouling and anti-icing coatings made from nanocellulose.

Nacre is a natural ceramic composite. Its microarchitecture is traditionally known as a "brick-bridge-mortar" arrangement. The bricks refer to flat polygonal crystals of aragonite, which provide strength. Numerous mineral bridges are encompassed in the organic layer. The mortar is a biological organic adhesive composed of polysaccharide and protein fibers, which provide ductility capacity and energy redistribution. The combination of soft biopolymer and hard aragonite makes nacre twice as strong and much tougher than its constituent materials [124,125]. Xu et al. [126,127] used a coiled-spring model to explain that the biopolymer matrix in nacre can strengthen itself during deformation; the authors also measured the elastic modulus (11 GPa) of the thin biopolymer matrix.

Inspired by the multiscale architecture of nacre, Guan et al. [96] prepared a high-performance sustainable structural material from CNF and TiO_2-coated mica micro platelets (TiO_2-mica) (Fig. 4A-E). A directional deforming assembly method was implemented to achieve a highly oriented brick-and-mortar structure.

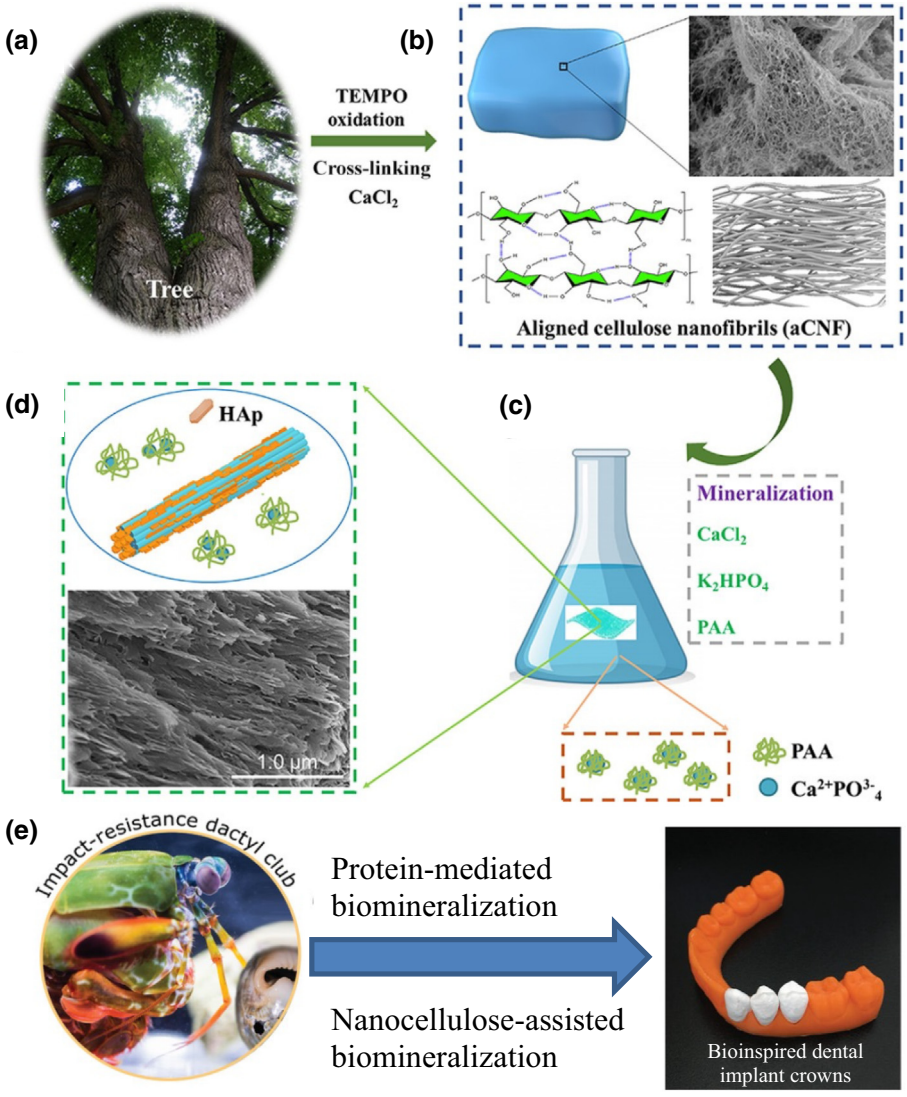

FIGURE 3

Schematic illustration of fabricating the mineralized nanocomposite. (A) Tree; (B) aligned CNF and its structure; (C) mineralization process; (D) mineralized aligned CNF composite (function: strong because elastic modulus is ~10 GPa; future application: scaffolds for repair and regeneration of hard tissues) and its scanning electron microscope image with an aligned mineralized structure [87]; and (E) bioinspired nanocomposite (function: strong because tensile strength is ~460 MPa; future applications: bone repair, bioengineering) that mimics key architectural and molecular features of the mantis shrimp dactyl club via biomineralization [91].

The carboxyl groups of CNFs were crosslinked by the Ca^{2+}, which led to a strong ionic bond network and improved the interaction between CNFs. The composite hydrogel was pressed to form a highly oriented 2D building block (i.e., brick) with a uniformly distributed 1D nano building block (i.e., mortar) between the bricks. The structure prepared using bioinspired materials and biomimetic design had better mechanical and thermal properties than conventional petroleum-based plastics.

Similarly, Qiu et al. [97] mimicked the brick-and-mortar microstructure of nacre and fabricated black phosphorus functionalized with hydroxyl groups (BP-OH)/CNF composite films via vacuum-assisted filtration self-assembly. 2D hydroxyl-functionalized BP-OH was the hard segment and acted as the brick, whereas 1D CNF was the soft segment and acted as the mortar. The CNF adhered to adjacent BP − OH nanoflakes and improved the friction energy dissipation and stress transfer efficiency. The nacre-inspired BP-OH/CNF composite film had strong interfacial hydrogen bonding between BP-OH and CNF, which resulted in a 300% increase in tensile strength compared with pure CNF film. Ultrathin flexible BP-OH/CNF composite films also demonstrated good flame resistance (peak heat release rate of ~50 W/g) and high thermal stability (decomposition temperature of ~290 °C), with potential application in flame-retarded insulation materials and flexible construction materials.

Hu et al. [98] prepared highly thermally conductive, electrically insulating, flexible, and superhydrophobic nanocellulose composite films via a dual-bioinspired (i.e., lotus leaf and nacre) design. The rough surface morphology of lotus leaves was imitated to attain super-hydrophobicity and self-cleaning properties. CNF/OH-BNNS films were prepared using vacuum-assisted

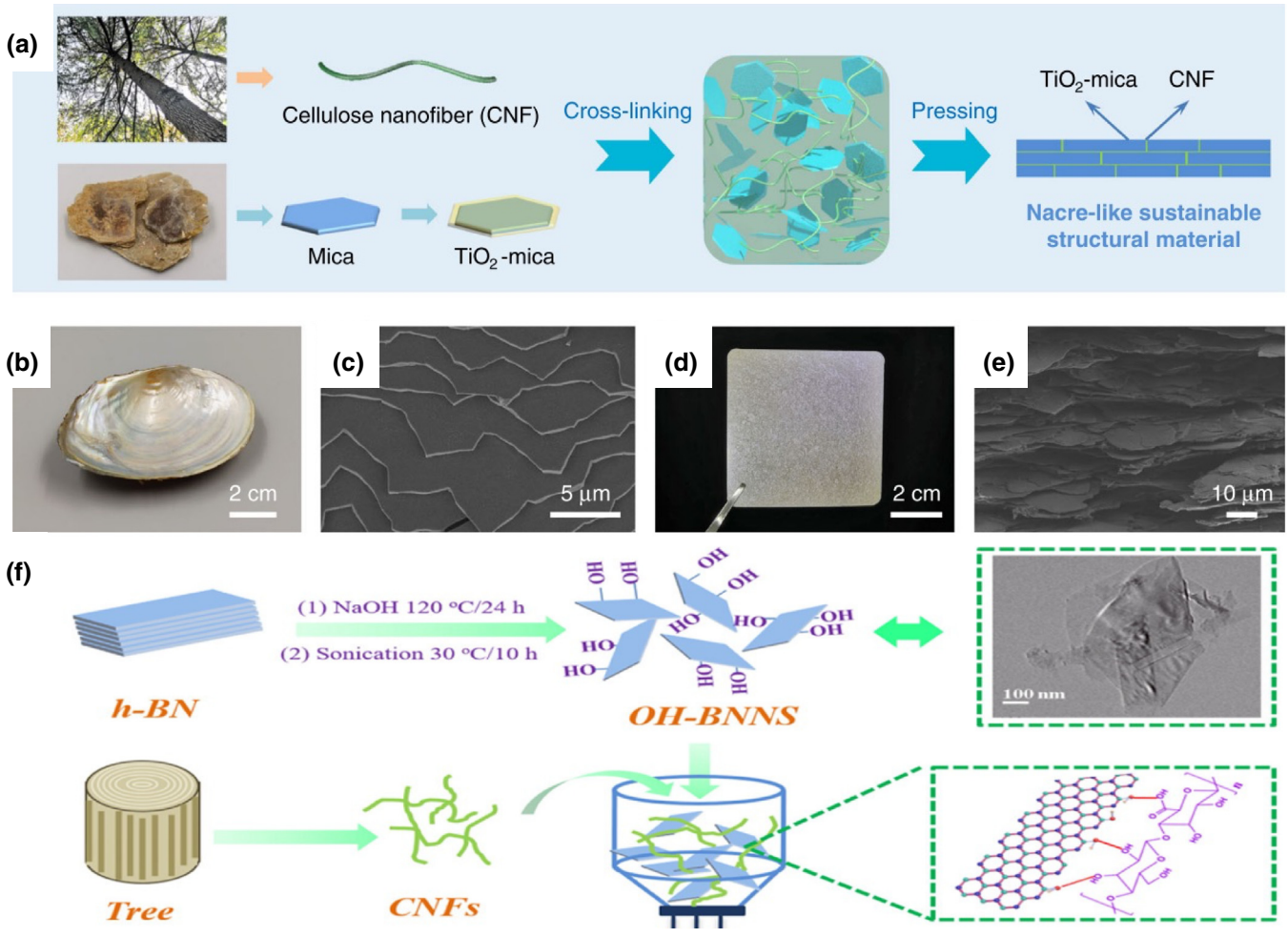

FIGURE 4

Preparation of natural bioinspired structural materials. (A) A schematic of the directional deforming assembly pathway to fabricate bioinspired high-performance structural materials; (B) nacre; (C) fracture surface of the nacre; (D) bioinspired structural material; (E) fracture surface of the bioinspired structural material (function: strong because of high strength [281 MPa], high toughness [11.5 MPa $m^{1/2}$], and high stiffness [20 GPa]; application: alternative structural material to substitute plastics) [96]; and (F) illustration of the preparation of OH-BNNS (boron nitride nanosheet) and CNF/OH-BNNS composite films (biomimetic design template: lotus leaf and nacre; functions: high thermal conductivity and excellent hydrophobicity; application: cooling electronic devices) [98].

assembly and were modified using a low–surface energy modifier of fluorinated silane molecules (Fig. 4F). The modified composite film showed excellent hydrophobicity with a contact angle larger than 155° and self-cleaning properties similar to a lotus leaf. Additionally, the morphology of the CNF/OH-BNNS (50 wt%) composite film depicted a highly oriented layered structure with 2D OH-BNNS tightly integrated with CNFs. The structure was analogous to a nacre-like brick-and-mortar structure. This highly oriented structure resulted in efficient heat dissipation along the in-plane direction and showed a 505% enhancement in thermal conductivity compared with pure CNF films.

Different biological composites such as bone, crustacean shells, and ivory have a helicoidal microstructural motif and have a hierarchical and periodic arrangement of hard and soft phases. Because of these microstructural properties, these composites are tough without being excessively ductile. Inspired by the helicoidal microstructure of these composites, Natarajan et al. [95] fabricated helicoidal CNC films with excellent mechanical properties using wood-derived CNCs and tunicate-derived CNCs. In most cellulose-rich helicoidal composites, wood-derived CNCs are used. Lower aspect ratios of wood-derived CNCs have shorter interaction lengths and poor shear transfer capabilities, leading to poor mechanical properties of the nanocomposites. To address this issue, Natarajan et al. used a length bi-dispersity strategy by adding high–aspect ratio tunicate-derived CNCs in low–aspect ratio wood-derived CNCs. This strategy resulted in improvement in effective overlap length that improved shear transfer efficiency and thus the modulus and strength of the film. Furthermore, the helicoidal architecture helped improve out-of-plane properties of the composites, such as bending modulus, hardness, and impact tolerance. The resulting materials could be applied as protective coatings. Overall, little literature specifically discusses the use of coating for the bioinspired design towards nanocellulose-based materials. In addition, it will be quite interesting to see other strategies (e.g., templating) used in this research field.

Nanocellulose functions and applications

Nanocellulose is a promising substrate for developing superhydrophobic materials because it is renewable, biodegradable, and has unique physical, chemical, and mechanical properties, unlike conventional substrates. The potential applications of superhydrophobic materials include automobile windshields, oil–water filtration, water-repellant packaging materials, self-cleaning clothing, microfluidic devices, and construction materials [109,128]. Beyond the hydrophobicity, nanocellulose exhibits other excellent properties such as adhesion, adsorption, and flame resistance. Based on these functions, nanocellulose has wide applications such as smart materials (e.g., stimuli-responsive material, shape memory polymer, sensor, actuator), composites, and biomedical engineering. Table 2 exhibits some representative differences between nanocellulose-based materials with specific functions.

Surface wetting

Super-hydrophobicity

Superhydrophobic materials have a static contact angle greater than 150° for water droplets. Nanocellulose has been shown to exhibit super-hydrophobicity (a water contract angle >150°) after proper treatments [129–131]. However, the intrinsic hygroscopicity of nanocellulose (without treatment) in general is a big challenge. Superhydrophobic surfaces designed using nanocellulose are mainly inspired by structural hierarchies similar to plant leaves or insect surfaces such as rose petals and lotus leaves or water strider legs, respectively [108–111]. Various chemical modification strategies are employed to enhance the hydrophobicity by tuning the surface chemistry and structural designs. Nanocellulose provides robust nanostructures and abundant hydroxyl groups for attaching low surface energy moieties such as fluorine and silane through mechanisms such as plasma deposition, chemical vapor deposition, sol–gel, and chemical etching.

Inspired by mimicking the hierarchical surface roughness and wetting properties of lotus leaves, Mertaniemi et al. [108] developed a superhydrophobic coating on a glass surface using silane–modified CNF microparticles. The superhydrophobic surface resulted in a static water contact angle higher than 150° due to the microstructure arrays and low surface energy of the surface. The materials can be used for self-cleaning applications. A similar approach was used by Zhang et al. [109] for coating commercial filter paper with CNF aerogel microspheres to obtain lotus leaf–like structured surface roughness. Subsequently, the filter paper was modified with silane copolymer to fabricate superhydrophobic filter paper. The modified filter paper showed efficient oil–water separation because of its water repellency. One possible mechanism is a thin layer of water formed on the original paper surface so that oil is repelled away from the paper surface. Klochko et al. [110] designed rose petal–based nanocellulose films by building hierarchical nanostructures of copper iodide onto cellulose paper. The hierarchical roughness of copper iodide provides a combination of high hydrophobicity with a large contact area, which enables high adhesion of droplets as on rose petals. These films can be applied for lab-on-a-chip microfluidic devices. Jin et al. [111] demonstrated that a nanocellulose aerogel carrier has some common features with the water striders, such as load-carrying on water. The nano- to microscale features of these superhydrophobic aerogels mimicked bristly water strider legs. The nanosized grooves trapped air between the aerogel and water surface and could withstand a few orders of magnitude greater weight than the weight of the aerogel itself. The nanocellulose aerogel has a density of 0.02 g/cm^3 and a porosity of 98.6%. One potential application for this material is gas-permeable, buoyant, and dirt-repellent coatings for sensors.

TABLE 2

Representative differences of nanocellulose-based materials with specific functions.

Material	Inspired design template	Mechanism of working	Functional performance	Ref.
Nanocellulose/$CaCO_3$	Nacre	Layer-by-layer assembly of nanocellulose films and controlled infiltration with liquid $CaCO_3$ precursors to generate lamellar materials	Strong (reduced Young's modulus of 14 GPa)	[6]
CNC/copolymer	Squid beak	Thiol − ene crosslinking with a copolymer through UV irradiation	Strong (storage modulus of 289 MPa)	[94]
CNF/OH-BNNS film	Lotus leaf and nacre	Highly ordered hierarchical architecture and strong hydrogen bonding interaction	Excellent hydrophobicity (contact angle of >155°)	[98]
CNF/dopamine/Fe	Mussel byssal thread	Coupling mechanism of CNF and dopamine via carbodiimide chemistry; swelling mechanism associated with Fe^{3+} ions	High adhesion (wet adhesion of −10 mN/m)	[2]
CNW-reinforced polyurethane	Sea cucumber dermis	Mechanically adaptive behavior and high elasticity of wet materials	Shape memory (55% shape memory effect upon exposure to water)	[100]
CNC/copolymer film	Beetle shell	CNC with structural color with left-handed helicity, and copolymer giving rise to the organic solvent–responsive structural color and wider red-shift window of the reflectance peak	Structural colors (color change from blue to yellow, regulated repeatedly under the stimulus of cyclohexanone)	[101]
Copper iodide–modified nanocellulose paper	Rose petal	Hierarchical structures of copper iodide onto nanocellulose, increasing surface roughness	Highly hydrophobic (water contact angle of 143°)	[110]

Nanocellulose's hydrophilic hydroxyl functionality can be easily modified to fabricate bioinspired nanocomposite designs similar to mussels or plant cell walls with higher water resistance, thereby improving their applicability in aqueous environment applications. Yao et al. [112] engineered the interface between CNF and montmorillonite for increased wet adhesion via partial conjugation of dopamine molecules onto CNF and reaction with montmorillonite, inspired by the versatile bio-adhesive capabilities of mussel adhesive proteins. The resultant nanocomposites exhibited excellent barrier and mechanical properties. The mechanical performance is improved because of the strong interfacial adhesion between the montmorillonite and CNF, caused by the conjugated dopamine molecules on CNF surfaces. The broad applications of the materials include tissue engineering and the encapsulation of drugs. Prakobna et al. [113] prepared core–shell CNF (amylopectin-coated CNF)-containing nanocomposites inspired by water-resistant properties of primary plant cell wall structures. The nanocomposites showed improved water resistance than pure amylopectin and CNF. The distribution of the amylopectin in thin CNF coatings causes amylopectin confinement as an interphase region next to rigid CNF nanofibers, thereby restricting the molecular mobility and hygroscopicity of amylopectin.

Superhydrophobic surface can also bring some other unique properties, such as self-cleaning and anti-icing. For example, mechanochemistry approaches have been used to fabricate functionalized nanocellulose to achieve bioinspired architectures for self-cleaning and anti-icing without compromising structural integrity or functional disruption [132]. The fabricated product was a nanocellulose/waterborne polyurethane composite aerogel with a density of 0.054 g/cm^3, as shown in Fig. 5A. The microstructures of the aerogel could be easily controlled by adjusting the nucleation driving for structure-adaptable multifunctionalities. Thus, the sample with a *Salvinia minima*–inspired structure could achieve an ultralow density of 0.05 g cm^{-3} with excellent properties, including super-hydrophobicity, self-cleaning, and anti-icing properties, which were further demonstrated by droplet tests. As shown in Fig. 5B–D, the water droplet on the aerogel surface slipped off immediately without forming any ice crystals, indicating the excellent anti-icing ability of the aerogel, which was further verified with a decrease of crystallization temperature to −19 °C (it was −15 °C for WPU: waterborne polyurethane). Furthermore, the droplets of coffee, and juice rolled off the surface of the aerogel completely because of its superhydrophobic feature. Fig. 5E shows the wettability comparison of the pristine and modified CNF composites containing OH-BNNS, indicating a superhydrophobic surface was successfully constructed after the modification of fluorinated silane molecules. In summary, nanocellulose can become hydrophobic after proper treatments. This provides a large opportunity for treated nanocellulose to reinforce hydrophobic biopolymers (e.g., polylactic acid, polybutylene succinate) with a high fiber/polymer interfacial adhesion.

Adhesion, flame resistance, and adsorption

When cellulose-based materials are applied as fillers in composites, poor interfacial adhesion between cellulose and the matrix may limit the properties of the composites. By applying a surface modification to the nanocellulose, the interfacial adhesion between the polymer matrix and nanocellulose can be improved. In Yan et al.'s research [133], the surface modified micro-fibrillated cellulose had an improved interfacial bonding with soy protein isolated adhesive than unmodified micro-fibrillated cellulose, where the shear strength was improved from 0.4 MPa (soy protein isolated adhesive) to 1.4 MPa (soy protein isolated adhesive with 10 wt% filler). The cellulose was induced to form multiple interactions with soy protein isolate to form a stable crosslinking system. To reinforce soy protein composites, CNF was functionalized with 3-aminophenylboronic acid, shown in Fig. 6A. The boronic acid group can form dynamic hydrogen bonding between the various groups on soy protein [134]. The improved hydrogen bonding resulted in higher tensile strength and toughness, and the boronic acid also improved the flame resistance (peak heat release rate of 52 W/g), antibacterial activity, and thermal stability (decomposition temperature of ~265 °C) because of its inherent chemical properties.

Karabulut et al. modified CNF with dopamine for further ionic coordination with Fe^{3+}, inspired by marine mussel byssal threads [2]. The interactions between CNF in an aqueous dispersion were adjusted by coupling CNF with dopamine. The presence of the dopamine-Fe^{3+} complex improved the wet adhesion ~3 fold compared with that without Fe^{3+}. The resulting coating could provide strong adhesion with various surfaces for coating applications. Fernandes et al. modified the surface of bacterial cellulose with 3-aminopropyltrimethoxysilane to obtain an NH_2-functionalized cellulose membrane [135]. Because of the presence of the free amino groups, the membrane showed an antibacterial property against *Escherichia coli* while staying non-toxic to human adipose-derived mesenchymal stem cells. This membrane may be useful for biomedical applications.

Hu et al. modified the surface of BNNS with ammonium polyphosphate to form hydrogen bonding with CNF [114]. After the vacuum-assisted filtration of BNNS-p-APP and CNFs, a nacre-like microstructure could be formed with a high in-plane thermal conductivity (9.1 W m^{-1} K^{-1}). The flame-retardant APP molecules were wrapped onto the surface of BNNS via electrostatic interaction, creating a strong hydrogen bonding interaction with CNF chains. Flame resistance was also observed because of the layered architecture that could suppress the release of combustible volatiles and oxygen penetration, shown in Fig. 6B-C.

Other studies examined modified cellulose with grafted chains for surface modification. For example, Tang et al. extracted the CNF from a pomelo peel and oxidized some hydroxyl groups to carboxyl groups with H_2O_2 [136]. The obtained carboxylated CNF was grafted with polyethyleneimine, so the free amino groups could adsorb dye molecules and heavy metal ions in an aqueous solution. The adsorption capacity of malachite green and copper ions was 530 and 74 mg/g, respectively, which provides an environmentally friendly approach for waste adsorption by cellulose. Lassoued et al. grafted glycidyl methacrylate from oxidized CNF, which was cast to transparent and foldable films [137]. With the addition glycerol as a plasticizer, the film from the CNF-glycidyl methacrylate was more hydrophobic and had higher tensile extension. Increased hydrophobicity benefits the compatibility of the modified CNF with poly(vinyl butyral). The composites of poly(vinyl butyral) and modified

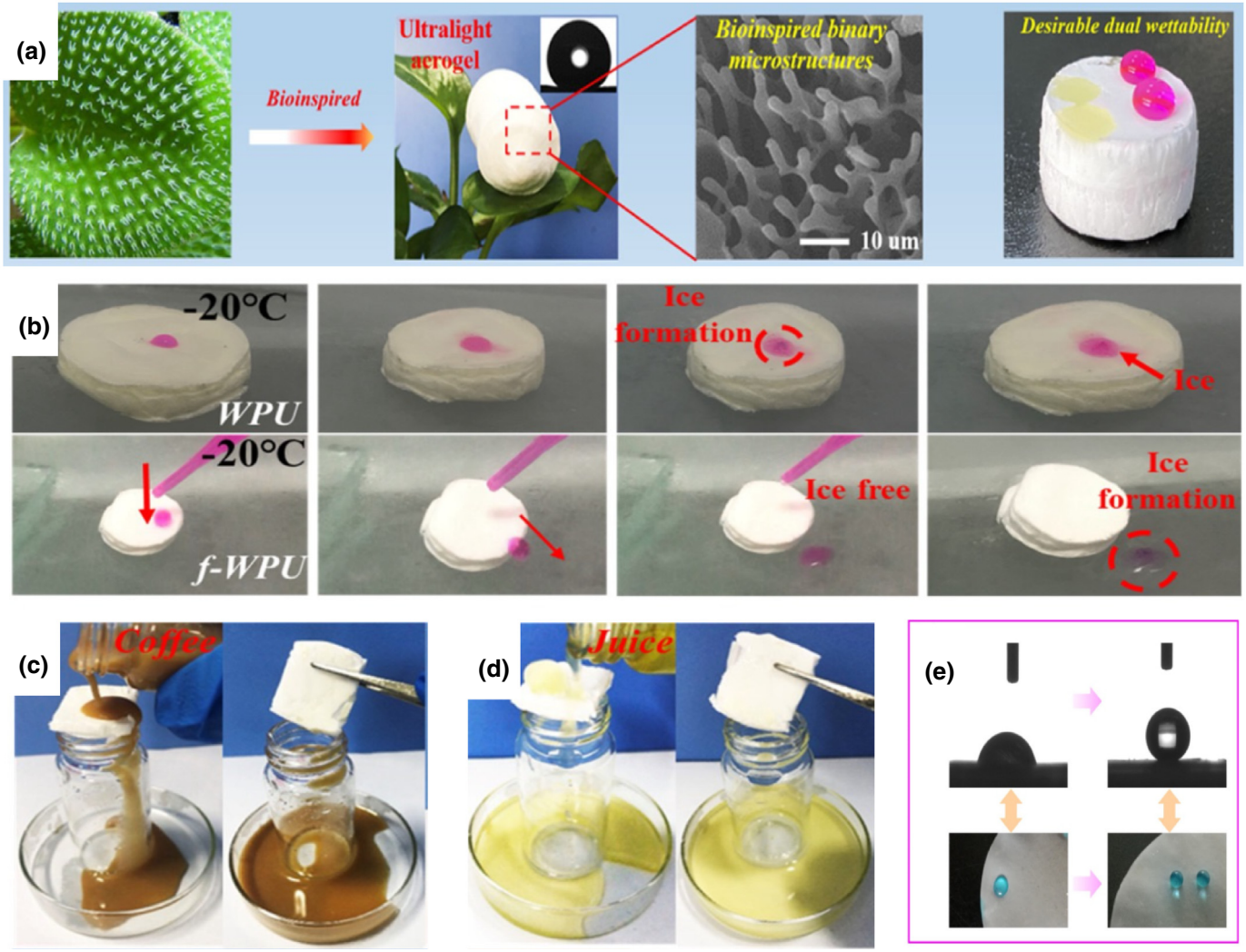

FIGURE 5

Functions of bioinspired nanocellulose-based materials. (A) Schematic illustration of *Salvinia minima*–inspired ultralight aerogels with desirable dual wettability; demonstration of (B) anti-icing and (C–D) self-cleaning properties of f-WPU (functionalized WPU; design strategy: assembly; application: self-cleaning coatings) [132]; and (E) static contact angle images of (left) pristine and (right) modified CNF/OH-BNNS composite membranes (biomimetic design template: lotus leaf and nacre; design strategy: assembly; application: cooling electronic devices) [98].

CNF have higher specific absorption energy than poly(vinyl butyral), which can potentially replace petroleum based poly (vinyl butyral) in safety glasses.

Liu et al. grafted CNC with quaternized side chains, which provides positively charged sites [138]. The brush-like, positively charged CNC had high efficiency for selective heparin capture, possibly because many free polymers in CNCs can capture heparin. The adsorption capacity reached ~41 mg/g at the first use and 37 mg/g after five rounds of capture and release, which is much higher than that of the commercial resin Amberlite-IRA900, which is 6 mg/g. Overall, nanocellulose exhibits different functions (e.g., adsorption, adhesion, flame resistance) after proper surface modification, inspired by nature. Among those functions, flame resistance becomes important regarding building material characteristics. Nanocellulose has attracted many researchers' attention because its incorporation into polymer composites could improve their thermal stability.

Smart materials

Stimuli-responsive material

Smart materials are a class of advanced materials that are manufactured to respond to external stimuli in a controlled method. As an example, some responses are stimuli-responsive because they can change properties in response to external stimuli. Property changes include changes in color, shape, state of matter, and texture, which can be triggered chemistry, pH, moisture, electric fields, magnetic fields, force, light, and temperature. Materials can also be programmed to be multi-responsive, where a range of external stimuli can be used to cause multiple changes within the material. Smart materials often mimic behaviors observed in nature. For example, sea cucumbers can selectively control their rigidity as a defense mechanism. This behavior is being exploited by researchers to develop a range of biomaterials [99,139].

A stimuli response can be triggered in nanocelluloses using properties inherent to the cellulose. This is most accomplished by exploiting the hydroxyl groups on the cellulose surface to

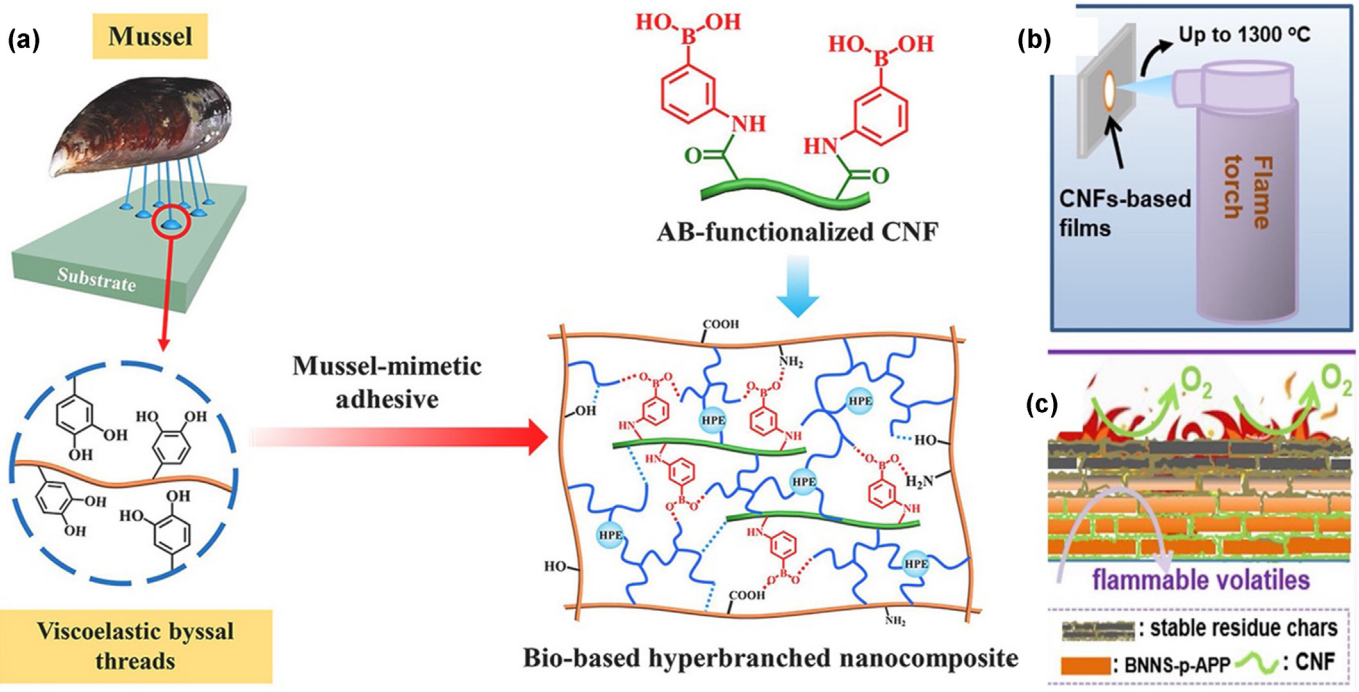

FIGURE 6

Fabrication and proposed mechanism of bioinspired nanocellulose-based materials. (A) Preparation process of a mussel-mimetic CNF-based nanocomposite adhesive with a proposed mechanism: dynamic covalent interactions and intermolecular sacrificial hydrogen bonds (AB-functionalized refers to 3-aminophenylboronic acid-functionalized; function: flame resistance and thermal stability; application: packaging) [134]; (B) schematic illustration of the flame-retardant test; and (C) schematic illustration of the possible flame-retardancy mechanism of CNF-based composite films (BNNS-p-APP: BNNS with ammonium polyphosphate; biomimetic design template: nacre; application: flexible electronics) [114].

change as a result in differences in pH, electric fields, chemistry, or temperature. For example, CNCs can be functionalized with pendant amine groups and utilized to make colloids that can change from solid to liquid-like behaviors from temperature changes [140]. Likewise, the extensive hydrogen bonding within CNCs can impart water-responsive properties (i.e., self-healing) to composite materials [141]. Depending on the polymer matrix within the composite and the specific chemistry utilized, shape memory can also be created in CNC composites, allowing for a change in shape as a response to stimuli [142–145].

Shape memory material

The use of the nanocellulose in shape memory polymers has been widely studied [99,100,142,146,147], but bioinspired nanocellulose-based shape memory polymers are limited, mainly focusing on water-activated shape memory polymer composites, in which nanocellulose is used as a reinforcing filler [99,100]. This inspiration of using nanocellulose as shape memory polymer composites comes from the ability of many echinoderms such as sea cucumbers to alter stiffness rapidly and reversibly (Fig. 7A-B). The dermis of sea cucumbers consists of rigid, high–aspect ratio, collagen fiber–reinforced nanocomposites, where the interaction between the reinforcement fillers can be regulated by chemical stimuli to alter stiffness. Following this principle, Capadona et al. [99] fabricated CNW–reinforced ethylene oxide–epichlorohydrin polymer, whose stiffness can be altered by water. The CNWs form a stiff percolating network in the nanocomposites through hydrogen bonding. The addition of water molecules can form competitive hydrogen bonds to disrupt the initial percolating network and thus soften the materials. The interactions between CNWs can be switched on (Fig. 7C, dry state) and off (Fig. 7D, wet state) changing the elastic modulus. The storage moduli of dry composites increased from ~3.7 MPa (neat ethylene oxide–epichlorohydrin polymer) to ~800 MPa (19 vol% whiskers) with the whisker content, suggesting the formation of a percolation network of the CNWs, which was supported by a percolation model calculation [99,148,149]. After swelling in water, the storage moduli reduced from ~800 to 20 MPa and recovered upon drying. The authors also demonstrated similar stiffness alteration behavior in CNW-reinforced poly(vinyl acetate).

Following a similar principle, Mendez et al. [100] developed water-triggered shape memory composites based on CNW-reinforced polyurethane (Fig. 7E-F), inspired by the function of the sea cucumber dermis. The ability to form a percolating network of CNWs was used to temporarily store elastic energy applied to the composites. Once the water trigger was applied, the stiff percolating network broke and released the elastic energy to facilitate shape recovery. As shown in Fig. 7F, after immersion in water, the fish lure specimen moves autonomously, returning slowly to its original shape. To realize this kind of shape memory behavior, the composites were first exposed to a wet environment to switch off the hydrogen bond between the fillers, and then substantially stretched into an intermediate shape. Once the composites were dried, the stiff cellulose network reformed, and the consolidated temporary shape was

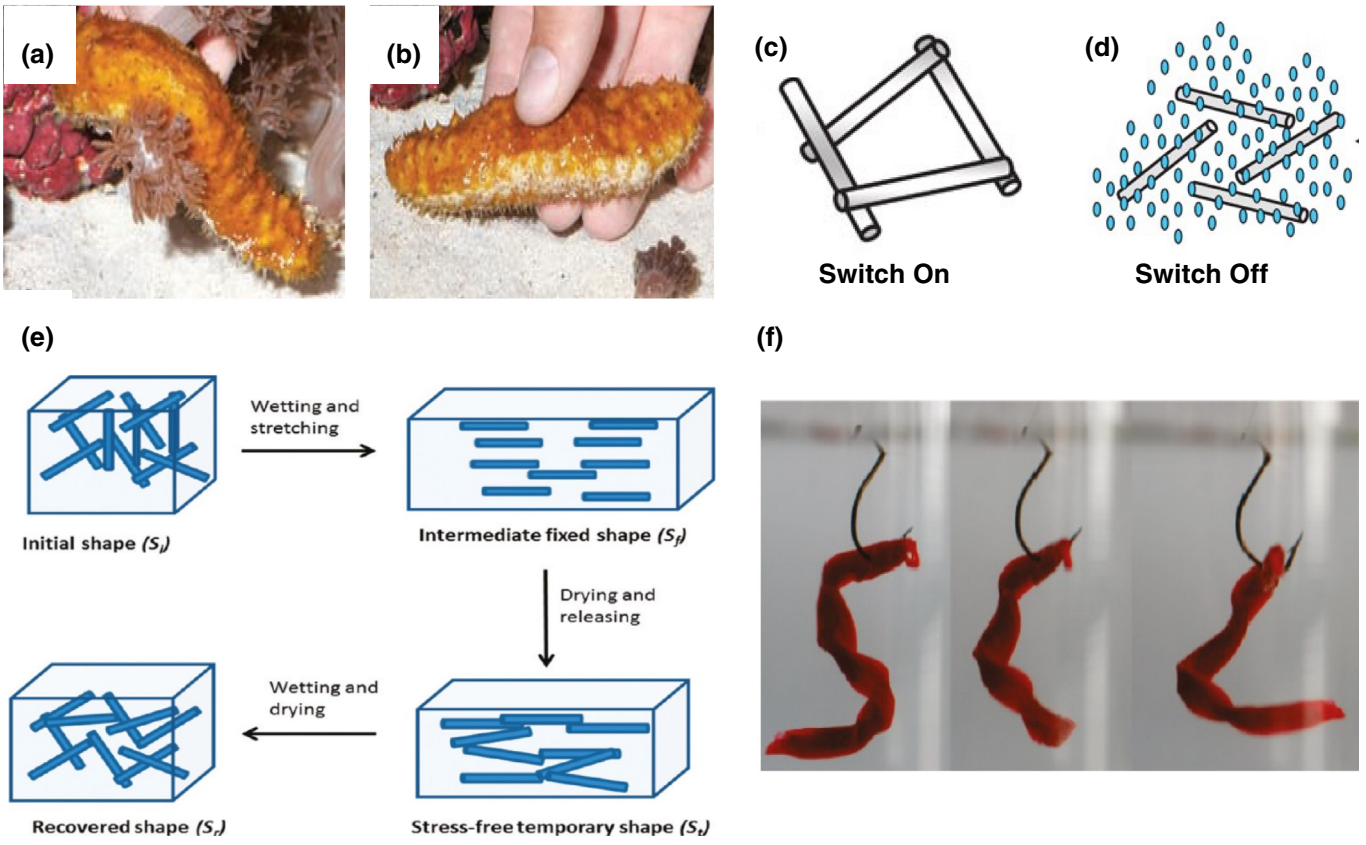

FIGURE 7

Shape memory of nanocellulose-based materials. Pictures of a sea cucumber in (A) relaxed and (B) stiffened states; schematics showing (C) the stiff percolating network of fibers generated in the dry state and (D) the lack of fiber interactions in the presence of water (design strategy: assembly) [99]; (E) schematic representation of the shape memory mechanism in CNW-reinforced polymer composites; and (F) water-triggered shape memory effect used in an artificial, self-propelled fishing lure (biomimetic design template: sea cucumber dermis; design strategy: assembly) [100].

obtained. Upon rewetting and drying, the composites recovered their initial shape. The team compared the shape memory behavior of the neat polyurethane and polyurethane/CNW nanocomposites comprising 20 vol% CNWs and found that neat polyurethane only had a marginal shape memory effect (1.5%) upon exposure to water, whereas the polyurethane/CNW had 55% shape memory effect. The shape memory behavior of polyurethane/CNW was observed in cyclic shape memory experiments. This principle has also been used in other studies to fabricate shape memory polymer composites, such as poly(vinyl acetate)/CNC [150], poly(glycerol sebacate urethane)/CNC [146], and rubber/CNC [151]. The primary chemical trigger is water, and future research may develop bioinspired nanocellulose-based shape memory polymers that respond to other triggers such as optical or electrical stimuli.

Sensing

Bioinspired nanocellulose-based materials and technologies have been engineered to possess sensing capabilities including photonic, gas/chemical, solvent, and strain sensing. In biochemistry, circular polarized light (CPL) is used as an information carrier for the vision of the stomatopod crustaceans [152]. Similarly, CPL can be used in modern information technology to relay information [153]. The self-assembly of CNC as it is dried from an aqueous suspension leads to a cholesteric nematic structure, which allows for the transmission of CPL and subsequent sensing/detection [154,155]. Grey et al. demonstrated the integration of a CNC film into amorphous indium-gallium-zinc oxide transistors for CPL sensing capabilities [154]. Others have also utilized cholesteric nematic structures, along with the available hydrogen bonding sites on the surface of the CNCs, to create bioinspired nanocomposites with custom mechanical and optical properties for photonic sensing applications [155].

Bioinspired nanocellulose-based materials have also been demonstrated as gaseous or chemical sensors. Researchers have incorporated nanocellulose into bioinspired solid, liquid, and gaseous sensors to detect chemistries such as urea, glucose, organic solvents, water, and hydrogen sulfide (H_2S). The detection of glucose and urea from a bioinspired nanocellulose-based sensor was demonstrated by Babitha et al., who fabricated a bioinspired ZnO nanoarchitecture using a series of biotemplates including carboxymethyl cellulose, resulting in the nonenzymatic electrochemical sensing of glucose and urea [156]. Others have shown the ability to detect specific liquids or whether a liquid state is present. For example, Sun et al. developed a structural color-changing film responsive to cyclohexane made from a copolymer blended with CNCs that mimicked the unique structural colors of beetle shells and butterfly wings (Fig. 8A-F) [101,157,158].

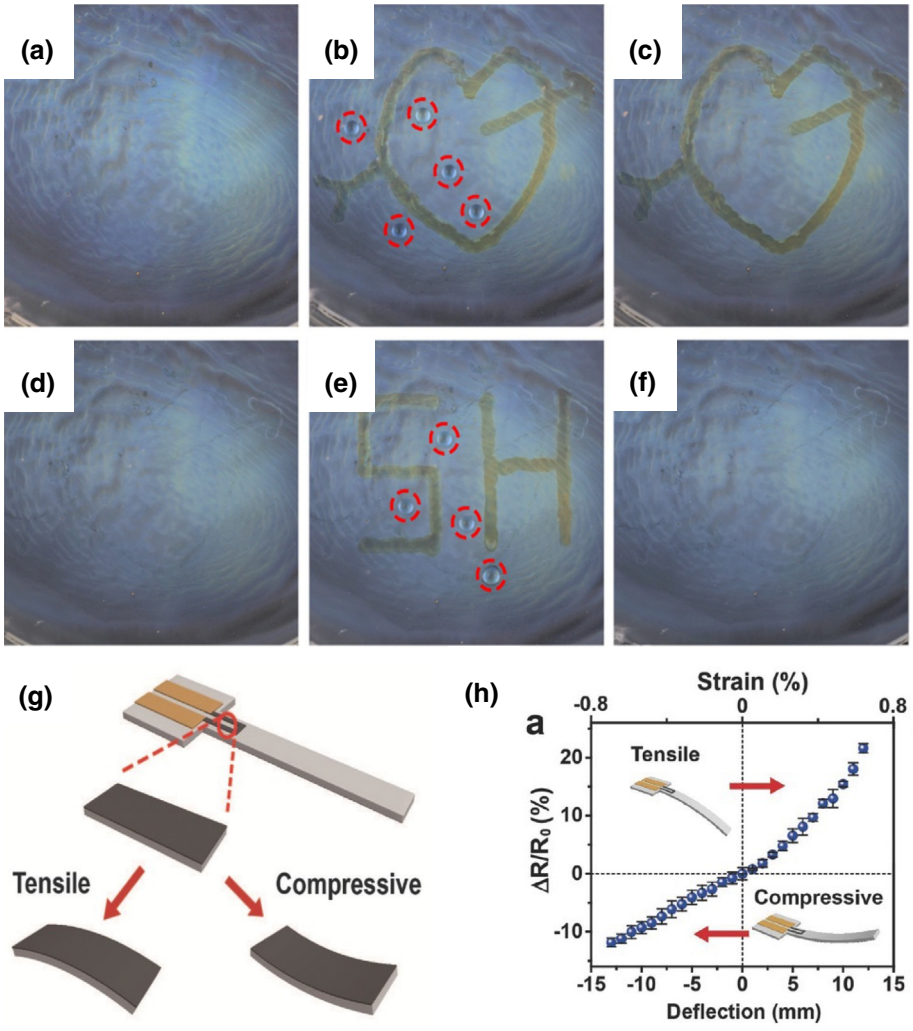

FIGURE 8

Example bioinspired nanocellulose-based sensors and actuators. (A) The neat PEG-PPG-PEG (polyethylene glycol-block-polypropylene glycol-block-polyethylene glycol) triblock copolymer/CNC film, (B, C) demonstrating the ability to sense organic solvent; (D–F) upon the evaporation of the organic solvent, the film returns to the original state. The dashed red circles indicate water droplets and demonstrate the hydrophobicity of the film (biomimetic design template: beetle shell and butterfly wing; design strategy: assembly) [101]; (G) schematic of the graphite pencil-traced/cellulose-based paper strain sensor; and (H) the ability of the sensor to detect strain in the form of resistance change as deflection occurs in tension or compression (R_0: initial resistance; ΔR: resistance change; biomimetic design template: human skin and rodent; design strategy: assembly) [103].

Zhang et al. harnessed inspiration from wood-like multicomponent structures to fabricate a CNF/carbon nanotube nanocomposite that act as a flexible liquid sensor that could detect the presence of water and ethanol [102]. Additionally, gaseous states can be detected by bioinspired nanocellulose containing sensors. For example, Kim et al. fabricated a H_2S sensor by functionalizing CNC and apoferritin onto tungsten trioxide (WO_3) nanotubes utilizing a bioinspired platinum catalyst that transitions to sodium tetra-tungstate ($Na_2W_4O_{13}$), granting the nanotube the ability to detect H_2S [159].

Researchers have developed nanocellulose-based sensors as easy-to-fabricate and easy-to-use strain sensors based on bioinspiration from human skin and rodent [103,160]. Hua et al. showed the ability of cellulose-based paper with a graphite (pencil) tracing on the surface to detect strain tension and compression during a cantilevered beam experiment **(**Fig. 8G-**H)** [103]. Microcracks can appear in neighboring graphite flakes when a tensile strain is applied, which causes an obvious increase in resistance. However, the neighboring graphite flakes can reconstruct overlaps when a compressive strain is applied, which decreases resistance. Nanocellulose has been incorporated into a wide variety of sensor types, including photonics and strain sensors, resulting from bioinspiration, all of which contribute to making sensing applications more renewable and sustainable.

Actuation

Examples of actuation as a result of response to a stimulus are abundant in nature and have been used as inspiration in conjunction with nanocellulose materials to engineer actuators mainly for soft robotic and wearable sensor applications [161]. Many different stimuli have been demonstrated to trigger a response of nanocellulose-based actuators. Common stimuli used for actuation are electricity, moisture, and temperature, and many actuators are activated by multiple stimuli

[85,104,105,161,162]. For example, Lv et al. developed a nanocellulose-based colloidal liquid metal capable of shape deformation as a result of an electrical or thermal stimulus based on the actuation of soft tissue [104]. A self-shadowing mechanism was proposed. When exposed to light, the photothermal heating of the liquid crystal network film and bending deformation toward the light were observed until the colloidal liquid metal–coated region was shadowed by the blank edge. The materials have potential applications in integrated soft electronics and bioinspired soft machines. The ability of motile plants to respond to temperature and humidity has also inspired the development of a flexible, porous, and freestanding actuator comprising a poly(vinyl alcohol-co-ethylene) substrate with a hydrophilic nanocellulose coating [105].

Actuators triggered by other stimuli besides electricity, temperature, and moisture have been developed for biomedicine, biomimetic machines, wearable sensors, and soft robotics. Hu et al. fabricated a light- and temperature-triggered actuating graphene-cellulose (paper) layered composite for potential integration into next-generation wearable sensors [160]. Whereas many of the aforementioned bioinspired nanocellulose-based actuators are layered nanocomposites, Duan et al. took inspiration from plant tissues to create hydrogels from chitosan and nanocellulose with the actuation capabilities depending on the pH value, demonstrating potential applications in biomedicine and biomimetic machines [106]. Overall, nanocellulose has been included in a wide variety of bioinspired actuators that respond to a large range of stimuli, primarily for biomimetic machines, soft robotics, and wearable sensors.

High mechanical performance composite

Nanocellulose offers the potential to develop composites that have high mechanical strength, toughness, and stiffness [13]. Mechanical properties are a crucial consideration in biomedical, automotive, and construction composites [163]. Brick-and-mortar assembly of natural nacre in mussels has long been a source of inspiration for producing strong nanocellulose composites. Natural nacre is a ternary composite of calcium carbonate ($CaCO_3$) in the aragonite phase, chitin, and protein. Nanofibrillar chitin in nacre controls biomineralization and mechanical strength [164]. Although the reinforcing mechanisms of incorporating nanocellulose in various composite systems was not clearly elucidated for every research article cited in this review, one study of mimicking nacre explained that nanocellulose could bridge cracks and resist montmorillonite platelets from sliding, thus enabling more montmorillonite platelets to slide in the following layer [92]. Such deformation behavior resulted in a toughened structure. In one study, montmorillonite platelets, CNF, and poly(vinyl alcohol) (PVA) were combined to produce an artificial nacre transparent composite through slow evaporation (Fig. 9A-D). The Young's modulus, tensile strength, and toughness reached 22.8 GPa, 302 MPa, and 3.7 MJ/m^3, respectively, owing to the layered and alternating structure of montmorillonite and CNF synergistic networks and interconnectivity by PVA [92]. These values are even higher than natural nacre, with 80–135 MPa tensile strength and 1.8 MJ/m^3 toughness [164]. In particular, the combination of these three components, especially nanocellulose, provides a good balance of strength, modulus, and toughness [92].

In nature, nacre has long been identified as an excellent natural armor, with high mechanical strength and toughness [166,167]. Li et al. [54] revealed that a single crystal-like aragonite platelet is assembled by screw dislocation and amorphous aggregation between aragonite nanoparticles. They further observed the formation of an aragonite nanoparticle self-assembly process and dome-shaped platelet formation. The improvements of nacre's strength and toughness are attributed to the dome-shaped platelet being stacked together to form an interlocking network against the sliding of the platelets [168]. A third-order lamellae was formed by aragonite nanoparticles, which served as the basic building blocks for the shell structure and contributed to the mechanical properties of the shell by buffering cracks and confining the damage to a relatively small volume [169]. The microlayers serving as integrated shields with different lamellar orientations are used to deflect and branch cracks between layers [170]. Curved reinforcements can also be used to construct conch spines, which exhibit a 30% increase in fracture strength compared to conch shell body parts [171].

Nacre-like composites can also be assembled by vacuum-based self-assembly of nanocellulose. Cai et al. [172] functionalized sodium alginate with dopamine simply by mixing. The addition of sodium alginate to CNC increased the tensile strength from 25.6 to 41.3 MPa and elastic modulus from 5.92 to 10.93 GPa in comparison to neat CNC. The functionalized sodium alginate provided more active –OH groups to form hydrogen bonding between the CNC matrix and functionalized sodium alginate. The presence of dopamine in these composites promoted interfacial adhesion that further increased the tensile strength to 48.4 MPa and elastic modulus to 12.8 GPa. The composites demonstrate good potential for fluorescent probe applications [172]. The composites' hydrogen bonding increased from 64% to 72% compared with neat CNC [173].

Biominerals are made of organic substances such as chitin and inorganic substances such as hydrated amorphous $CaCO_3$. The ratios of organic and inorganic substances control flexibility and transparency. For example, exoskeletons of crustaceans have high flexibility owing to their high organic content [93]. Kuo et al. [93] made a crustacean exoskeleton–mimicking transparent and flexible composite by combining CNF and carboxymethyl cellulose (CMC) with ACC and PAA. The crosslinking of Ca^{2+} ions with anionic groups in CMC and CNF gave the biomineral-inspired composite high mechanical strength. Furthermore, CMC/CNF/ACC had a Young's modulus of 15.8 GPa and tensile strength of 268 MPa, whereas a CMC/CNF film had a Young's modulus of 10.7 GPa and tensile strength of 240 MPa [93]. In another approach, ACC/PAA was percolated in oxidized bacterial nanocellulose, which provided freestanding yet flexible and tough films that could fully recover to their original state after flexural load was released. By binding ACC/PAA with nanocellulose, the tensile strength of the composite was 169 MPa and the elastic modulus was 7.3 GPa, whereas the *Marsupenaeus japonicas* exoskeleton had a tensile strength of 42 MPa and elastic modulus of 2.9 GPa (Fig. 9E-F) [165].

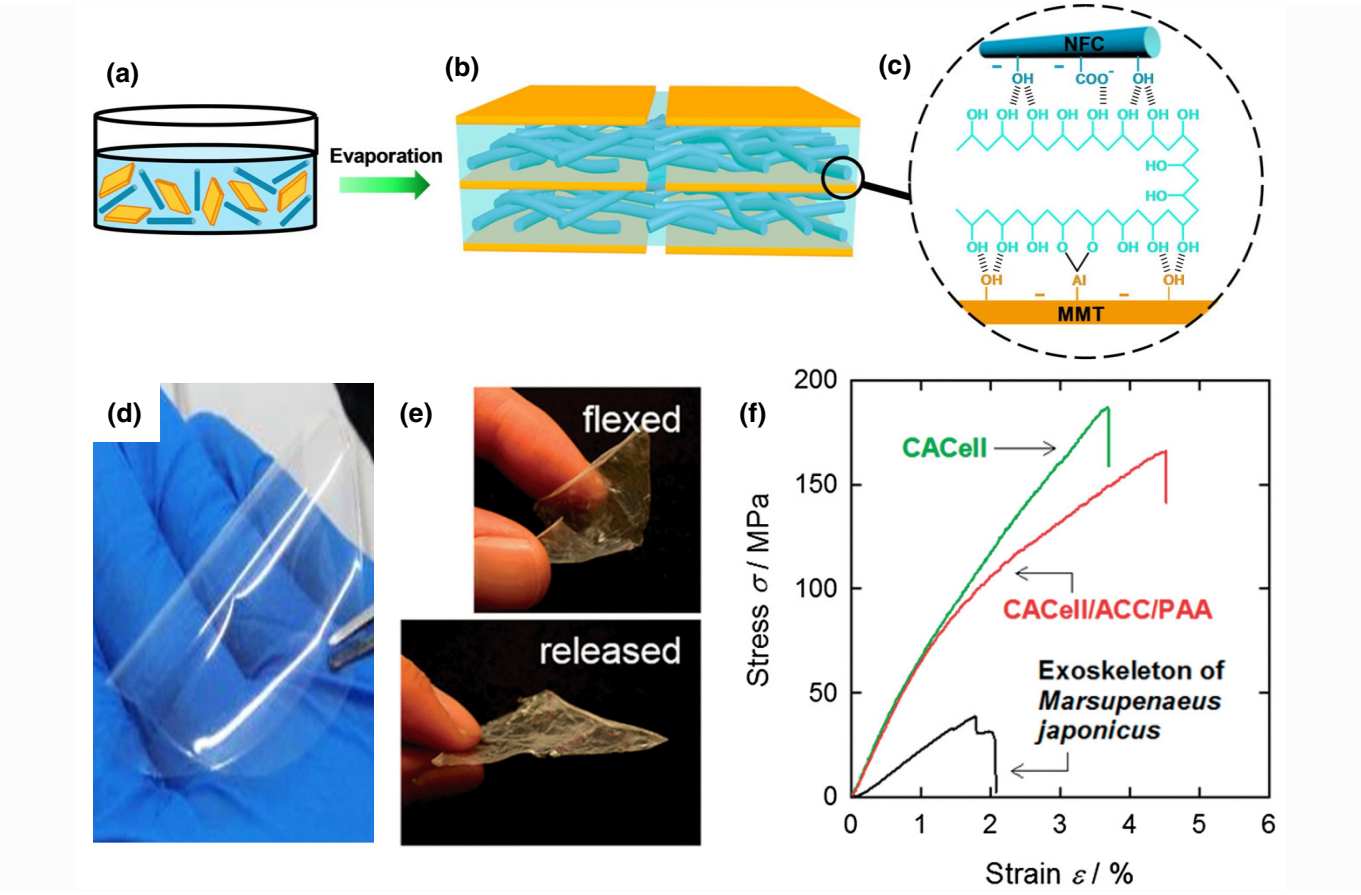

FIGURE 9

Nanocellulose-based composites with high mechanical performance. (A) Fine aqueous dispersion of montmorillonite platelets, CNF, and PVA; (B) proposed structural model for the artificial nacre, in which montmorillonite platelet and CNF fibril network layers are alternately stacked into a layered structure; (C) anionic montmorillonite platelets and anionic CNF fibrils are interconnected by PVA through hydrogen bonds and Al–O–C bonds, resulting in high tensile properties (MMT: montmorillonite); (D) digital photo of artificial nacre, showing a high level of transparency (application: precision optical devices, flexible electronics, and food packaging) [92]; (E) elastic flexibility of the CACell/ACC/PAA composites. The composite films with thicknesses ~10 μm are flexible, and the flexed films quickly revert to the original flat state after removing the flexural loading; and (F) tensile test: typical stress–strain curves of the CACell/ACC/PAA composite, neat CACell, and exoskeleton of *Marsupenaeus japonicas* (CACell: surface-carboxylated CNF; ACC: amorphous $CaCO_3$; PAA: polyacrylic acid; biomimetic design template: crustacean exoskeleton) [165].

Humboldt squid beak contains chitin nanofibers embedded in a protein matrix in which crosslinking and hydration can vary the elastic modulus from 5 GPa in the stiff beak to 50 MPa in the soft end connecting to muscles. The stiff portion contains hydrophobic histidine-rich proteins crosslinked with chitin, and the soft portion contains hydrated chitin with a low concentration of proteins. Materials with similar mechanical gradients are of value as orthopedic implants, and the properties of the Humboldt squid beak were mimicked using functionalized CNC crosslinked with a copolymer through UV irradiation. A storage modulus contrast of 20 could be achieved, and it could be varied from 14 to 289 MPa by tuning the degree of crosslinking [94].

The biocompatibility of cellulose makes it an attractive material for making high-performance composites [174]. Huang et al. prepared bone scaffolds using CNC/hydroxyapatite/chitosan composites through layer-by-layer assembly [175]. CNCs contain sulfate groups that bond to Ca^{2+} and PO_4^{3-} to form hydroxyapatite, and the hydroxyapatite content can be controlled by the pH of a simulated body fluid [176]. Presence of hydroxyapatite in the composites increased the Young's modulus from 6.5 to 9 GPa [175].

Zou et al. [177] studied the nanoscale structure of bamboo fibers and discovered the cobble-like polygonal cellulose nanograins present in the cell wall of the bamboo fibers, which act as the basic building block to form the individual fibers. These cellulose nanograins of bamboo fibers provide stiffness and act as reinforcements to the parenchyma cell wall (matrix). The hierarchical organization of these bamboo fiber bundles, parenchyma cells, and vascular bundles contribute to the excellent strength, stiffness, and toughness of bamboo [178]. Tao et al. [179] constructed TaC nanowire–activated carbon microfiber hybrid structures via a one-step carbothermal method using bamboo fibers, where bamboo fibers acted as a carbon source as well as the template. This hybrid structure derived from bamboo demonstrated strong potential for energy storage applications because its hierarchical heterostructures exhibited high capacitance and the nanowires showed high Young's modulus. Tao et al. [180] reported a bamboo-based carbothermal technique to prepare nanowires of interstitial carbides (e.g., TiC) and covalent

carbides. Nanoporous bamboo can be used as both the renewable carbon source and the template.

In another study by Tao et al. [181], radially aligned B_4C nanowires on carbon microfibers were developed using the porous cotton fiber obtained from a commercial cotton T-shirt, where cotton fibers acted as the carbon source and the template. The developed B_4C nanowires had low density, high aspect ratio, and high strength, whereas the carbon microfibers had higher modulus, making the nanowire/carbon microfibers hybrid structure an ideal candidate for mechanical reinforcement for lightweight composite systems. Similarly, TiC nanorods were synthesized on carbon microfibers using cotton fibers of a T-shirt [182]. The resulting material exhibited excellent Young's modulus of 432 GPa and had the prospect of being used as reinforcements of composites.

Long-term durability of several such biomimetic composites has not yet been tested and needs considerable attention. Biomimetic CNF–natural mica hydrogels with brick-and-mortar assembly were manufactured to serve as replacements to conventional plastics such as polymethylmethacrylate, acrylonitrile–butadiene styrene, polyamide, and polycarbonate. While the dimensions of the commercial plastics changed significantly between −130 °C and 150 °C, there were few changes in the dimensions of CNF–mica composites in this entire temperature range. The coefficient of thermal expansion of CNF-mica composites ($\sim 7 \times 10^{-6} K^{-1}$ at 25 °C) was at least 10 times lower than that of the commercial plastics. This may improve long-term stability because of lower instances of the buildup of mechanical stresses on thermal fluctuations [96]. In one study on biomimetic bone scaffolds, the long-term stability of extracellular matrix scaffolds made from Ca^{2+}-oxidized CNFs was tested for the proliferation of pre-osteoblast cells and compared with a natural extracellular matrix (a mixture of collagen, laminin, and other proteins) derived from a tumor cell line (Matrigel). The high porosity of CNF scaffolds resulted in significantly higher cell proliferation, cell stability, and mechanical stability over 3 weeks in comparison to Matrigel [183].

Biomimetic foams (inspired by the parenchyma cells that may have 10–50 μm diameter and <3 μm cell wall thickness) have also been produced by adding CNF in a starch matrix and freeze drying, resulting in cell sizes in the range of 20–70 μm. The size of ice crystals was controlled by the rate of freeze drying—high rates produced smaller pore sizes for making microcellular foam structures. Above 40% CNF reinforcement, the cell structures became elongated and had random orientation. By increasing the CNF content from 0% to 40%, the tensile strength was increased from 170 kPa to 510 kPa at 40%, and the Young's modulus was increased from 4.9 MPa to 7.0 MPa [107]. Overall, there are two major challenges regarding nanocellulose-based composites for large-scale applications: nanocellulose drying with a low cost and uniform dispersion of nanocelluloses in the polymer resin. Freeze drying can help preserve the fibril structure and reduce the fiber agglomeration, but it is a costly process. Other drying methods (e.g., spraying drying, oven drying) need to be further explored and developed.

The following is a brief summary of nanocellulose functions of other bioinspired design sources. Specifically, resilin-like polypeptides had terminal cellulose binding modules, which can adhere to nanocellulose. Genetically engineered resilin fusion proteins can also modify cellulose surfaces with an increased modulus of stiffness through a crosslinking effect in cellulose hydrogel and nanopaper [184]. Fungi including *Trichoderma* sp. and *Aspergillus* sp. are commonly used for the pretreatment of cellulosic biomass for the production of nanocellulose. A recent discovery in this area is controlled hydrolysis by fungi bypassing the homogenization process step [185]. Bacterial nanocellulose and fish gelatin composite displayed good adhesion and proliferation [186]. Mussel-inspired anisotropic nanocellulose and silver nanoparticle composites have also been found to have improved mechanical properties, electrical conductivity, and antibacterial activity [187].

Biomedical and oil absorbency applications

Many tissues in the human body, including muscles and blood vessels, are hierarchically ordered composite structures and exhibit highly anisotropic mechanical strength. This anisotropic structure plays key functions in tissue engineering, especially after suffering injury [188]. For example, Domingues et al. developed anisotropically aligned electrospun nanofibrous scaffolds with the assistance of nanocellulose as reinforcing fillers. The incorporation of a small amount of nanocellulose (up to 3 wt %) into tendon mimetic nanofiber bundles resulted in a significant biomaterial-toughing effect and enhanced the scaffolds' mechanical properties [189]. Tissue engineering has received widespread interest because it can repair damaged tissues effectively, creating artificial tissues to replace damaged parts and restore their original function [190]. Most commonly, the hydrogel/cellulose system has been selected as a potential invasive alternative for tissue engineering to promote a functional tissue healing process. Different types of nanocellulose can be employed as the matrix of hydrogel scaffolds for tissue engineering. To satisfy the requirements of different tissues, strategies including the use of crosslinking agents and additives have been established to produce nanocelluloses with controllable mechanical properties and tailorable biocompatibilities.

Massive blood loss is one of the primary causes of death from a wound, and creating antibacterial hemostatic materials with superabsorbent capacity is highly desirable [191]. Liu et al. [192] prepared a hydrogel sponge with hydroxyethyl cellulose/silica foam for hemostasis applications and antibacterial investigations. The hydrogel demonstrated superabsorbent capability by rapid water-triggered expansion, thus quickly reducing blood component (e.g., red blood cell, platelet) concentration. With the addition of silica foam (9.8 wt%), the modified hydrogel had an efficient hemostasis ability owing to the activated coagulation factors. Moreover, the hydrogel presented good antibacterial properties and excellent cytocompatibility after an ammonium group modification. Given these merits, the hydrogel could enable healing in a full-thickness skin defect model *in vivo*.

The flexible nature of hydrogen bonds in CNF could make them connect and break during structural deformation [193]. This feature can modulate its formation energy and offer the constructed materials with extraordinary properties, providing a possible strategy for mimicking the healing ability of natural tissues. As presented in Fig. 10A, a healed hydrogel consisting of tannic

acid–PVA/CNC could lift a weight of 100 g after the introduction of the tannic acid solution (15 wt%). The tannic acid-treated hydrogel achieved a stress of 1.4 MPa and a fracture strain of 215%. The hydrogel was fabricated based on multiple hydrogen bonds, and the rupture and reformation of the hydrogen-bonded network offered an efficient energy dissipation mechanism. These results revealed that the hydrogel could obtain self-recoverability owing to the reversible hydrogen bonds via the introduction of tannic acid. Furthermore, the hydrogel exhibited better healing performance after the addition of Fe^{3+} ions, lifting a weight of 200 g. This phenomenon is ascribed to the coupling effects of hydrogen bonds and coordination bonds within hydrogels. Thus, multi-bonds within hydrogel could promote its healing behaviors, presenting good self-recoverability.

Cytotoxicity plays an important function in practical applications. A prepared hydrogel's cytocompatibility can be determined by calculating the attached cell number and comparing its proliferation morphology. Researchers demonstrated that tannic acid-PVA/CNC hydrogels exhibit good biocompatibility and excellent antibacterial properties [193]. The tannic acid-PVA/CNC hydrogel is an ideal candidate for tissue engineering because of its excellent biocompatibility and antibacterial performance.

In addition to the functions and applications discussed above, nanocellulose-based materials could also be used for oil absorbency. Food and textile industries generate large volumes of oily wastewater daily, and these wastewaters, along with the frequent oil spill accidents from the petroleum industry, have become an ecosystem and health concern that requires immediate attention. Nanocellulose-based materials have great potential for oily wastewater treatment because of their high porous framework and large surface area. Cai et al. successfully prepared a WPU aerogel using functionalized nanocellulose as a structural, functional, and topographical modifier to mimic the surface of *Salvinia minima*, or floating ferns [132]. The resulting hydrophobic material showed great soybean oil absorbency ability (e.g., 60 g/g) owing to dual wettability, high porosity, and topologically controllable hierarchy, shown in Fig. 10B-C. A more elaborate discussion on the application of nanocellulose-based materials in oil field chemistry can be found elsewhere [194,195]. In summary, nanocellulose based hydrogels have potential in biomedical applications. However, continuous validation of nanocelluloses' response *in vivo* is needed for the hydrogels to be safely applied.

Conclusions

Summary

As a sustainable feedstock, nanocellulose can be integrated into bioinspired materials, leading to multifunctional properties such as surface-cleaning, anti-icing, water resistance, adhesion resistance, and stimuli response. Many designs are inspired by nacre (exhibiting exceptional toughness and strength), mussels (exhibiting remarkable strength, crosslinking, and adhesion), fish,

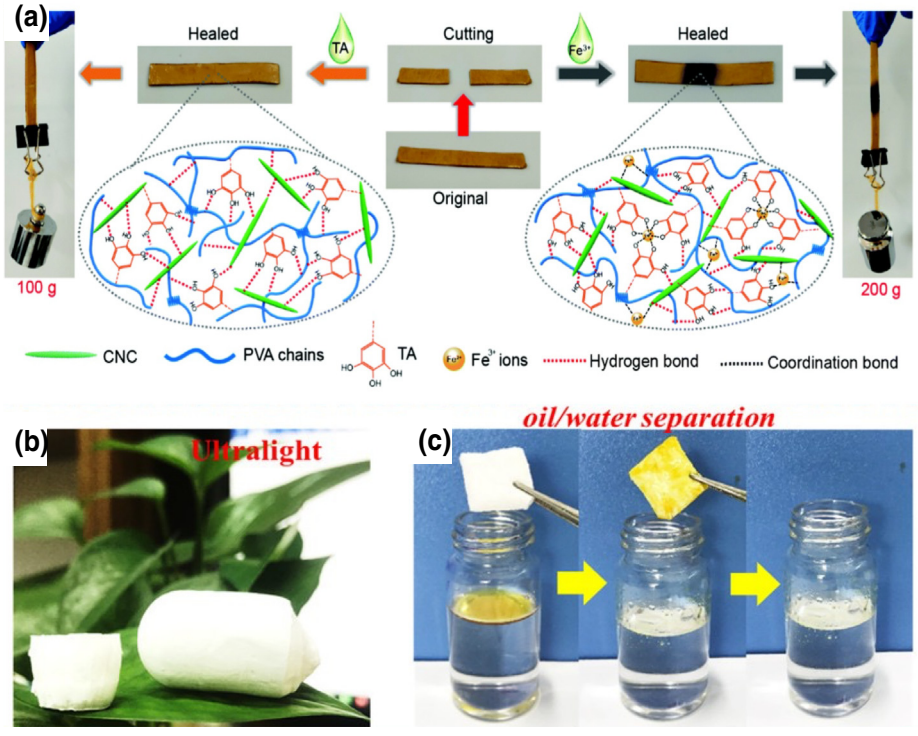

FIGURE 10

The healing ability or oil absorbance of nanocellulose-based materials. (A) Demonstration of tannic acid solution (15 wt%) and Fe^{3+} solution (0.3 mol/L)–assisted healing process of the tannic acid-PVA/CNC hydrogel and its possible mechanisms (TA: tannic acid; biomimetic design template: natural biological protein; design strategy: assembly; application: tissue engineering and biomedical) [193]; (B) optical picture of the ultralight aerogels; and (C) oil/water separation using the aerogel, indicating its high oil absorbance performance (biomimetic design template: *Salvinia minima*; design strategy: assembly; application: self-cleaning coating, oil removal) [132].

flies, and plants. The main strategies to apply bioinspired designs include biomineralization, coating, and self-assembly. Biomineralization can improve the mechanical properties of cellulose-based materials, while self-assembly of nanocellulose can lead to sensing/detection abilities because of its cholesteric nematic structure.

The major applications of bioinspired nanocellulose-based materials include composites for automotive applications, tissue engineering, stimuli-responsive materials, and oil absorbency. The nanocellulose-based composites have typical tensile strength of 26–302 MPa, Young's modulus of 1–23 GPa, and toughness of 4–36 MJ/m^3. The mechanisms behind bioinspired designs have been summarized: the shape memory mechanism in nanocellulose-based composites mainly includes wetting/stretching, drying/releasing, and wetting/drying. Sea cucumbers can selectively control their rigidity based on a defense mechanism, and chitosan-nanocellulose hydrogels swell based on an actuating mechanism.

Challenges and future directions

Fundamental research on bioinspired design and compatibility is needed to improve the functions of nanocellulose-based materials, as shown in Fig. 11. Some strategies, such as biomineralization and self-assembly, have been developed to improve the mechanical properties of composites, but the mechanisms behind this property enhancement have not been deeply studied. The intrinsic hygroscopicity of nanocellulose must be addressed via proper methods. Incorporation of nanocellulose in polymers has challenges such as incompatibility with hydrophobic polymers and strong hydrogen bonding among nanocellulose fibers, which causes flocculation. When cellulose-based materials are applied as fibers in composites, the interfacial adhesion between the cellulose and the matrix may limit the composite performance. Modifying the surface wetting of nanocellulose is a promising method for improvement.

Like for many new materials intended for industrial applications, standards and regulations are still in development for nanocelluloses. Although advances have been made by the Technical Association of the Pulp and Paper Industry, and the Canadian Standards Association, discrepancies still need to be addressed for the wide implementation of nanocelluloses in value-added products. One of the main concerns that slow the development of international regulations is the limited knowledge on nanocellulose safety. The size of nanocelluloses is in the same scale as the main regulator of cellular, which could enable a more direct interaction.

Cost reduction of nanocellulose-based materials needs to be explored for bioinspired designs. Fibrillation and other mechanical processes are energy-demanding, and the production of nanocelluloses are not yet competitive against fossil-based polymers. A low cost can be maintained by using sustainable biomass residuals and developing cost-effective nanocellulose production processes. The wide variability and wide application of nanocellulose, and how nanocellulose can be a promising solution to the development of bioinspired materials are also technical challenges.

In the future, fundamentally understanding how different natural systems work and the origin of their functionalities is vital. Developing new ways to generate nanocellulose and understanding how to improve the functions of nanocellulose-based materials toward targeted applications are crucial for bioinspired designs. Nanocellulose mixing with other immiscible liquid phases enables the formation of emulsions and resulting composites after the liquid is removed from the media. These properties allow for nanocellulose suspensions to be sought after for applications such as active coatings and food additives. In addition, bioinspired nanocellulose-based shape memory polymers and packages can be explored more. Furthermore, incorporating

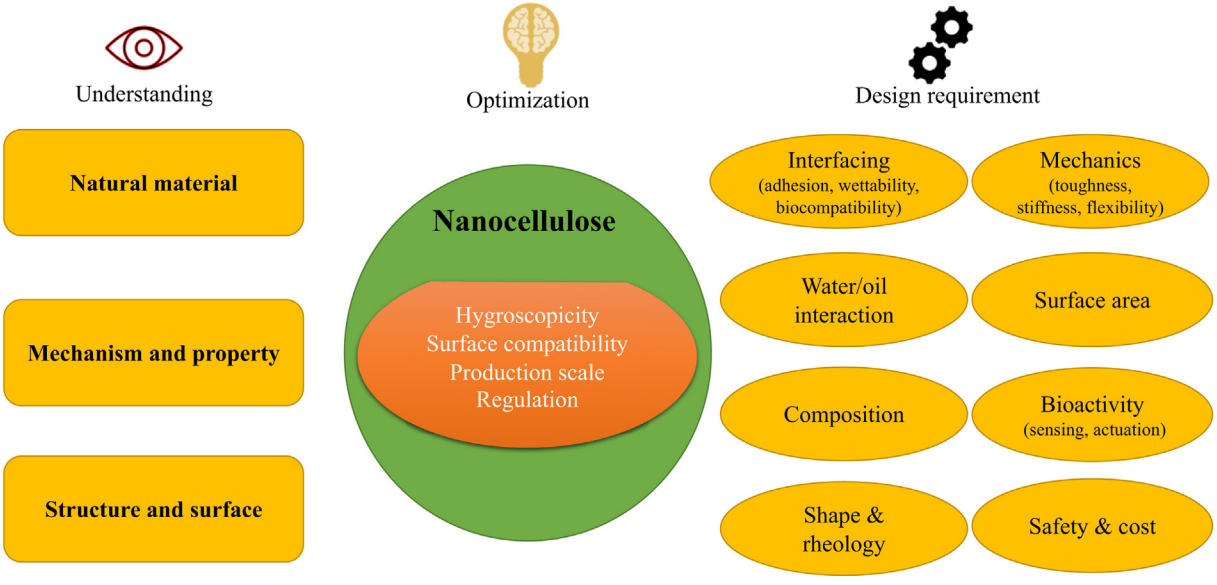

FIGURE 11

Overall research direction and the need for bioinspired nanocellulose-based materials.

functional additives (e.g., inorganic particles and biopolymers) in nanocellulose is a promising approach to increase its mechanical performance (e.g., toughness) and application.

CRediT authorship contribution statement

Xianhui Zhao: Conceptualization, Writing – original draft, Writing – review & editing. **Samarthya Bhagia:** Writing – original draft, Writing – review & editing. **Diego Gomez-Maldonado:** Writing – original draft, Writing – review & editing. **Xiaomin Tang:** Writing – original draft, Writing – review & editing. **Sanjita Wasti:** Writing – original draft, Writing – review & editing. **Shun Lu:** Writing – original draft, Writing – review & editing. **Shuyang Zhang:** Writing – original draft, Writing – review & editing. **Mahesh Parit:** Writing – original draft, Writing – review & editing. **Mitchell L. Rencheck:** Conceptualization, Writing – original draft, Writing – review & editing. **Matthew Korey:** Writing – original draft, Writing – review & editing. **Huixin Jiang:** Writing – original draft, Writing – review & editing. **Jiadeng Zhu:** Writing – original draft, Writing – review & editing. **Xianzhi Meng:** Writing – original draft, Writing – review & editing. **Meghan E. Lamm:** Conceptualization, Writing – original draft. **Katie Copenhaver:** Writing – review & editing. **Maria S. Peresin:** Writing – review & editing. **Lu Wang:** Writing – review & editing. **Halil Tekinalp:** Conceptualization, Writing – review & editing. **Guang Yang:** Writing – review & editing. **Vipin Kumar:** Writing – review & editing. **Gang Chen:** Writing – review & editing. **Kashif Nawaz:** Writing – review & editing. **X. Chelsea Chen:** Writing – review & editing. **Uday Vaidya:** Writing – review & editing. **Arthur J. Ragauskas:** Writing – review & editing. **Erin Webb:** Writing – review & editing, Funding acquisition. **Douglas J. Gardner:** Writing – review & editing. **Ping He:** Writing – original draft. **Ximin He:** Writing – review & editing. **Kai Li:** Conceptualization, Writing – original draft, Writing – review & editing. **Soydan Ozcan:** Conceptualization, Writing – review & editing, Funding acquisition.

Data availability

Data will be made available on request.

Declaration of Competing Interest

The authors declare that they have no known competing financial interests or personal relationships that could have appeared to influence the work reported in this paper.

Acknowledgments

The authors acknowledge the support from the US Department of Energy (DOE), Office of Energy Efficiency and Renewable Energy, Advanced Manufacturing Office under CPS Agreement 35714, Bioenergy Technologies Office, and Building Technologies Office. Credit of Graphical Abstract images: photographer Yao Qian and Li Li. This manuscript was authored in part by UT-Battelle LLC under contract DE-AC05-00OR22725 with DOE. The US government retains and the publisher, by accepting the article for publication, acknowledges that the US government retains a nonexclusive, paid-up, irrevocable, worldwide license to publish or reproduce the published form of this manuscript, or allow others to do so, for US government purposes. DOE will provide public access to these results of federally sponsored research in accordance with the DOE Public Access Plan (http://energy.gov/downloads/doe-public-access-plan).

References

[1] B.L. Tardy et al., Chem. Rev. 121 (22) (2021) 14088.
[2] E. Karabulut et al., ACS Nano 6 (6) (2012) 4731.
[3] B.K. Ahn, J. Am. Chem. Soc. 139 (30) (2017) 10166.
[4] S.Q. Cui et al., ACS Sustain. Chem. Eng. 8 (16) (2020) 6363.
[5] P. Das et al., ACS Appl Polym Mater 1 (6) (2019) 1505.
[6] M. Farhadi-Khouzani et al., J. Mater. Chem. A 5 (31) (2017) 16128.
[7] D.J. Zhu et al., Adv. Eng. Mater. 14 (4) (2012) B185.
[8] J.H. Waite, C.C. Broomell, J. Exp. Biol. 215 (6) (2012) 873.
[9] K. Copenhaver et al., Cellul. 29 (9) (2022) 4835.
[10] M.C. Iglesias et al., For. Prod. J. 70 (1) (2020) 10.
[11] S. Lombardo, W. Thielemans, Cellul. 26 (1) (2019) 249.
[12] B. Medronho et al., Cellul. 19 (3) (2012) 581.
[13] K. Copenhaver et al., ACS Sustain. Chem. Eng. 9 (40) (2021) 13460.
[14] K. Li et al., J. Mater. Sci. 57 (17) (2022) 8127.
[15] L. Wang et al., Compos Part B-Eng 201 (2020) 108297.
[16] J.Y. Zhu et al., Biotechnol. Biofuels 14 (1) (2021) 114.
[17] I. Usov et al., Nat. Commun. 6 (2015) 7564.
[18] K. Uetani et al., Sci. Rep. 11 (1) (2021) 790.
[19] R.M. Parker et al., Adv. Mater. 30 (19) (2018) e1704477.
[20] O.R. Juárez-Rivera et al., Appl. Sci. 11 (13) (2021) 6191.
[21] Q. Wu et al., Carbohydr. Polym. 235 (2020) 115962.
[22] S. Rajala et al., ACS Appl. Mater. Interfaces 8 (24) (2016) 15607.
[23] L. Csoka et al., ACS Macro Lett. 1 (7) (2012) 867.
[24] L. Zhai et al., ACS Appl Bio Mater 3 (7) (2020) 4329.
[25] L. Wang et al., Biomacromolecules 22 (10) (2021) 4037.
[26] K. Li et al., Carbohydr. Polym. 256 (2021) 117525.
[27] S. Wang et al., Prog. Polym. Sci. 53 (2016) 169.
[28] D. Mohan et al., Polymers (Basel) 12 (9) (2020) 1876.
[29] X. Qiu, S. Hu, Materials (Basel) 6 (3) (2013) 738.
[30] S.H. Hassan et al., J. Renewable Mater. 6 (1) (2018) 1.
[31] S. Ummartyotin, H. Manuspiya, Renew Sust Energ Rev 41 (2015) 402.
[32] P. Saha et al., ACS Appl. Mater. Interfaces 10 (28) (2018) 24116.
[33] R.J. Moon et al., Chem. Soc. Rev. 40 (7) (2011) 3941.
[34] D. Klemm et al., Adv. Polym. Sci. 205 (1) (2006) 49.
[35] X. Xu et al., ACS Appl. Mater. Interfaces 5 (8) (2013) 2999.
[36] C. Somerville, Annu. Rev. Cell Dev. Biol. 22 (2006) 53.
[37] J. Pennells et al., Cellul. 27 (2) (2019) 575.
[38] E.J. Foster et al., Chem. Soc. Rev. 47 (8) (2018) 2609.
[39] Y. Song et al., Angew. Chem. Int. Ed. Engl. 57 (42) (2018) 13838.
[40] Y. Wang et al., Carbohydr. Polym. 168 (2017) 112.
[41] K.V. Pillai, S. Renneckar, Biomacromolecules 10 (4) (2009) 798.
[42] T. Utzig et al., Angew. Chem. Int. Ed. 55 (33) (2016) 9524.
[43] T.L. Coombs, P.J. Keller, Aquat. Toxicol. 1 (5–6) (1981) 291.
[44] Y. Wang et al., Macromolecules 53 (11) (2020) 4568.
[45] H. Zhao, J.H. Waite, J. Biol. Chem. 281 (36) (2006) 26150.
[46] J.H. Waite, Integr. Comp. Biol. 42 (6) (2002) 1172.
[47] V.V. Papov et al., J. Biol. Chem. 270 (34) (1995) 20183.
[48] M.H. Ryou et al., Adv. Mater. 23 (27) (2011) 3066.
[49] H. Lee et al., P Natl Acad Sci USA 103 (35) (2006) 12999.
[50] X.H. Wang et al., ACS Appl Polym Mater 1 (11) (2019) 2998.
[51] U.G.K. Wegst et al., Nat. Mater. 14 (1) (2015) 23.
[52] J.W. Dunlop, P. Fratzl, Annu. Rev. Mat. Res. 40 (2010) 1.
[53] Z.W. Huang et al., Sci. Rep. 1 (2011) 5.
[54] X.D. Li, Z.W. Huang, Phys. Rev. Lett. 102 (7) (2009) 4.
[55] X.D. Li et al., Nano Lett. 4 (4) (2004) 613.
[56] Z.W. Huang et al., J. Mater. Res. 29 (14) (2014) 1573.
[57] H.Z. Li et al., Nano Lett. 14 (5) (2014) 2578.
[58] X. Li, JOM 59 (2007) 71.
[59] X.D. Li et al., Nano Lett. 6 (10) (2006) 2301.
[60] Z.W. Huang, X.D. Li, Sci. Rep. 3 (2013) 6.
[61] D.E. Moulton et al., Proc. Natl. Acad. Sci. 117 (1) (2020) 43.
[62] N. Song, Science,, et al., Advances 6 (42) (2020) eaba7016.
[63] X. Tao et al., Adv. Mater. 20 (21) (2008) 4091.
[64] N. Funk et al., Acs Appl Mater Inter 7 (10) (2015) 5972.
[65] J.D. Fox et al., J. Am. Chem. Soc. 135 (13) (2013) 5167.
[66] G.K. Qin et al., Nat. Commun. 3 (2012) 1003.
[67] J. Zhang et al., Langmuir 25 (3) (2009) 1371.

[68] M. Wu et al., Angew. Chem. Int. Ed. Engl. 53 (13) (2014) 3358.
[69] Z. Guo, W. Liu, Plant Sci. 172 (6) (2007) 1103.
[70] T. Sun et al., Acc. Chem. Res. 38 (8) (2005) 644.
[71] Q.F. Guan et al., Nano Lett. 21 (2) (2021) 952.
[72] D. Liu et al., Carbohydr. Polym. 75 (1) (2009) 39.
[73] Y. Zhang, Z. Guo, Chem. Lett. 43 (7) (2014) 1137.
[74] J.R. Capadona et al., Science 319 (5868) (2008) 1370.
[75] J.A. Trotter et al., Matrix Biol. 15 (2) (1996) 99.
[76] K. Shanmuganathan et al., Prog. Polym. Sci. 35 (1–2) (2010) 212.
[77] K. Liu et al., J. Am. Chem. Soc. 143 (2) (2021) 1162.
[78] A. Choi et al., J. Mater. Chem. A 9 (29) (2021) 15937.
[79] E. Cudjoe et al., ACS Cent. Sci. 3 (8) (2017) 886.
[80] L. Li et al., Angew. Chem. Int. Ed. Engl. 60 (18) (2021) 10186.
[81] J. Cui et al., Biomacromolecules 13 (3) (2012) 584.
[82] Z.K. Wang et al., ACS Macro Lett. 5 (2) (2016) 220.
[83] Z.K. Wang et al., ACS Nano 9 (1) (2015) 271.
[84] Z. Zou et al., Sci. Adv. 4 (2) (2018). eaaq0508.
[85] Z. Sun et al., J. Electrochem. Soc. 167 (4) (2020) 047515.
[86] L.A. Estroff, Chem. Rev. 108 (11) (2008) 4329.
[87] Y. Qi et al., ACS Appl. Mater. Interfaces 11 (31) (2019) 27598.
[88] V. Prasad Shastri, MRS Bull. 40 (6) (2015) 473.
[89] N.K. Dhami et al., Front. Microbiol. 4 (2013) 314.
[90] S.K. Bhadada, S.D. Rao, Calcif. Tissue Int. 108 (1) (2021) 32.
[91] P. Mohammadi et al., Adv. Mater. 33 (42) (2021) e2102658.
[92] J. Wang et al., ACS Nano 8 (3) (2014) 2739.
[93] D. Kuo et al., ACS Omega 3 (10) (2018) 12722.
[94] Y. Zhang et al., Biomacromolecules 22 (1) (2021) 201.
[95] B. Natarajan et al., Adv. Funct. Mater. 28 (26) (2018) 1800032.
[96] Q.F. Guan et al., Nat. Commun. 11 (1) (2020) 5401.
[97] S. Qiu et al., ACS Appl. Mater. Interfaces 12 (32) (2020) 36639.
[98] D. Hu et al., ACS Appl. Mater. Interfaces 12 (9) (2020) 11115.
[99] R. Capadona Jeffrey et al., Science 319 (5868) (2008) 1370.
[100] J. Mendez et al., Macromolecules (Washington, DC, U. S.) 44 (17) (2011) 6827.
[101] C. Sun et al., Appl. Mater. Interfaces 12 (2020) 26455.
[102] C. Zhang et al., Appl. Mater. Interfaces 12 (2020) 55527.
[103] Q. Hua et al., Adv. Electron. Mater. 2 (7) (2016) 1600093.
[104] P. Lv et al., Mater. Horiz. 8 (2021) 2475.
[105] Q. Zhu et al., Appl. Mater. Interfaces 11 (2019) 1440.
[106] J. Duan et al., Soft Matter 13 (2017) 345.
[107] A.J. Svagan et al., Adv. Mater. 20 (7) (2008) 1263.
[108] H. Mertaniemi et al., RSC Adv. 2 (7) (2012) 2882.
[109] F. Zhang et al., Cellul. 24 (7) (2017) 2913.
[110] N. Klochko et al., Cellul. 28 (14) (2021) 9395.
[111] H. Jin et al., Langmuir 27 (5) (2011) 1930.
[112] K. Yao et al., ACS Appl. Mater. Interfaces 9 (23) (2017) 20169.
[113] K. Prakobna et al., Biomacromolecules 16 (3) (2015) 904.
[114] D. Hu et al., Carbohydr. Polym. 264 (2021) 118058.
[115] Y.Z. Wan et al., Compos. Sci. Technol. 66 (11) (2006) 1825.
[116] E.B. Duarte et al., Cellul. 22 (5) (2015) 3177.
[117] N. Reznikov et al., Science 360 (6388) (2018) eaao2189.
[118] X. Zhang et al., J. Mater. Chem. 18 (6) (2008) 621.
[119] U. Mock et al., J. Phys. Condens. Matter 17 (9) (2005) S639.
[120] X. Gao, L. Jiang, Nature 432 (7013) (2004) 36.
[121] G.E. Fogg, Nature 154 (3912) (1944) 515.
[122] I.S. Bayer, Adv. Mater. Interfaces 7 (13) (2020) 2000095.
[123] Q. Wang et al., J. Mater. Chem. 20 (16) (2010) 3211.
[124] F. Song et al., Biomaterials 24 (20) (2003) 3623.
[125] H.W. Zhao et al., NPG Asia Mater. 10 (2018) 22.
[126] Z.H. Xu, X.D. Li, Adv. Funct. Mater. 21 (20) (2011) 3883.
[127] Z.H. Xu et al., Mater. Sci. Eng. C-Mater. Biol. Appl. 31 (8) (2011) 1852.
[128] C. Li et al., Adv. Funct. Mater. 26 (33) (2016) 6121.
[129] I.I. Smalyukh, Adv. Mater. 33 (28) (2021) e2001228.
[130] P. Das et al., Sci. Rep. 7 (2017) 39910.
[131] F. Chen et al., ACS Appl. Mater. Interfaces 12 (49) (2020) 55501.
[132] C. Cai et al., ACS Appl. Mater. Interfaces 12 (9) (2020) 11273.
[133] Q. Yan et al., J. Appl. Polym. Sci. 137 (39) (2020) 49176.
[134] K. Li et al., Compos. B Eng. 219 (2021) 108943.
[135] S.C. Fernandes et al., ACS Appl. Mater. Interfaces 5 (8) (2013) 3290.
[136] F. Tang et al., Chem. Eng. J. 395 (2020) 125070.
[137] M. Lassoued et al., Carbohydr. Polym. 254 (2021) 117411.
[138] Q. Liu et al., Chem. Eng. J. 420 (2021) 129811.
[139] D. Li et al., ACS Appl. Mater. Interfaces 12 (1) (2020) 1549.
[140] F. Azzam et al., Biomacromolecules 11 (12) (2010) 3652.
[141] L. Song et al., Macromolecules 50 (19) (2017) 7475.
[142] M.E. Lamm et al., Polymer 144 (2018) 121.
[143] Z. Wang et al., ACS Macro Lett. 5 (5) (2016) 602.
[144] Y. Li et al., ACS Appl. Mater. Interfaces 7 (23) (2015) 12988.
[145] Y. Liu et al., ACS Appl. Mater. Interfaces 7 (7) (2015) 4118.
[146] T. Wu et al., Biomacromolecules 15 (7) (2014) 2663.
[147] Y. Lu et al., Cellul. 28 (3) (2021) 1469.
[148] J.R. Capadona et al., Nat. Nanotechnol. 2 (12) (2007) 765.
[149] M.A.S. Azizi Samir et al., Biomacromolecules 6 (2) (2005) 612.
[150] K.L. Dagnon et al., Macromolecules 46 (20) (2013) 8203.
[151] M. Tian et al., ACS Appl. Mater. Interfaces 9 (7) (2017) 6482.
[152] T.-H. Chiou et al., Curr. Biol. 18 (2008) 429.
[153] Y.K. Takahashi et al., Phys. Rev. Appl 6 (2016) 054004.
[154] P. Grey et al., Adv. Funct. Mater. 29 (21) (2019) 1805279.
[155] B. Zhu et al., Appl. Mater. Interfaces 8 (2016) 11031.
[156] K.B. Babitha et al., Materials Advances 1 (6) (2020) 1939.
[157] Y. Habibi et al., Chem. Rev. 110 (2010) 3479.
[158] P. Tseng et al., Nat. Nanotechnol. 12 (2017) 474.
[159] D.H. Kim et al., ACS Sens 3 (6) (2018) 1164.
[160] Y. Hu et al., J. Mater. Chem. C 7 (2019) 6879.
[161] H. Deng et al., J. Mater. Chem. B 6 (34) (2018) 5415.
[162] T. Wu et al., J. Mater. Chem. C 4 (2016) 9687.
[163] K. Li et al., ACS Appl Polym Mater 2 (2) (2020) 411.
[164] R.Z. Wang et al., J. Mater. Res. 16 (2021) 2485.
[165] T. Saito et al., Mater. Horiz. 1 (3) (2014) 321.
[166] Z. Huang, X. Li, Phys. Rev. Lett. 109 (2) (2012) 025501.
[167] J. Liu et al., Phys. Rev. Lett. 118 (10) (2017) 105501.
[168] G.S. Zhang, X.D. Li, Cryst. Growth Des. 12 (9) (2012) 4306.
[169] H.Z. Li et al., J. Struct. Biol. 184 (3) (2013) 409.
[170] X.D. Li, P. Nardi, Nanotechnology 15 (1) (2004) 211.
[171] H.Z. Li, X.D. Li, J. Bionic Eng. 16 (4) (2019) 711.
[172] C. Cai et al., Cellul. 27 (17) (2020) 10241.
[173] E. Žagar, J. Grdadolnik, J. Mol. Struct. 658 (3) (2003) 143.
[174] X. Zhao et al., Resour Conserv Recy 177 (2022) 105962.
[175] C. Huang et al., Carbohydr. Polym. 222 (2019) 115036.
[176] C. Huang et al., RSC Adv. 9 (10) (2019) 5786.
[177] L. Zou et al., Mater. Sci. Eng. C 29 (4) (2009) 1375.
[178] L. Zou, X. Li, JOM 73 (6) (2021) 1705.
[179] X. Tao et al., Adv. Energy Mater. 1 (4) (2011) 534.
[180] X. Tao et al., J. Mater. Chem. 21 (25) (2011) 9095.
[181] X. Tao et al., Adv. Mater. 22 (18) (2010) 2055.
[182] X. Tao et al., Cryst. Growth Des. 11 (10) (2011) 4422.
[183] H.J. Kim et al., Cellul. 25 (12) (2018) 7299.
[184] W. Fang et al., Biomacromolecules 18 (6) (2017) 1866.
[185] N. Vigneshwaran, P. Satyamurthy, in: Advances and Applications Through Fungal Nanobiotechnology, Switzerland, Springer, Cham, 2016, p. 321.
[186] L. Bao et al., Polymers (Basel) 14 (20) (2022) 4367.
[187] H.L. Nguyen et al., Polymers (Basel) 8 (3) (2016) 102.
[188] J. Xing et al., Adv. Funct. Mater. 32 (15) (2021) 2110676.
[189] R.M. Domingues et al., Adv. Healthc. Mater. 5 (11) (2016) 1364.
[190] J.C. Courtenay et al., Cellul. 24 (1) (2017) 253.
[191] L. Zheng et al., Chem. Eng. J. 416 (2021) 129136.
[192] C. Wang et al., ACS Appl. Mater. Interfaces 11 (38) (2019) 34595.
[193] F. Lin et al., J. Mater. Chem. B 8 (18) (2020) 4002.
[194] X. Wang et al., ACS Omega 6 (32) (2021) 20833.
[195] S. Fürtauer et al., Polymers 13 (16) (2021) 2739.